

KfK 4111
August 1986

Theory of Mode Interaction in the Gyrotron

G. S. Nusinovich
Institut für Kernphysik

Kernforschungszentrum Karlsruhe

KERNFORSCHUNGSZENTRUM KARLSRUHE

Institut für Kernphysik

KfK 4111

THEORY OF MODE INTERACTION IN THE GYROTRON

G.S. Nusinovich *

Lectures presented during a visit to the Institut für Kernphysik II,
Kernforschungszentrum Karlsruhe, October, 1984

Kernforschungszentrum Karlsruhe GmbH, Karlsruhe

* Institute of Applied Physics, Academy of Sciences of the USSR, Gorky, USSR

Als Manuskript vervielfältigt
Für diesen Bericht behalten wir uns alle Rechte vor

Kernforschungszentrum Karlsruhe GmbH
Postfach 3640, 7500 Karlsruhe 1

ISSN 0303-4003

ABSTRACT

A nonlinear theory of multimode gyrotrons is developed, which describes such effects as mode competition (ie suppression of unexcited modes by the operating one), nonlinear excitation of passive modes by the active one, and mode locking. Mode competition is the dominant effect for modes with close frequencies (relative to the cyclotron resonance band). In such a system only single mode oscillations are stable. Nonlinear excitation of passive modes whose frequency is greater than the frequency of the operating mode is possible due to electrons under the action of the operating mode group in the decelerative phase with respect to the passive modes. For three or more modes with an equidistant spectrum of frequencies, mode locking takes place when the beam current substantially exceeds the threshold conditions, even though one mode finds itself in the nonlinear excitation band. The results obtained permit one to estimate the conditions for stable single mode oscillation in multimode gyrotrons.

THEORIE DER MODE-KONKURRENZ IM GYROTRON

ZUSAMMENFASSUNG

Eine nichtlineare Theorie eines mehrmodigen Gyrotrons wird vorgestellt, die solche Effekte wie Mode-Konkurrenz (die Unterdrückung einer nicht angeregten Mode durch die Betriebsmode), die nichtlineare Anregung einer passiven Mode durch die schon angeschwungene und Mode-Locking beschreibt. Der wichtigste Effekt für Moden mit eng benachbarten Frequenzen nah an der Zyklotronresonanz ist die Mode-Konkurrenz. Nur einzelne Moden können stabil in ein solches System schwingen. Die nichtlineare Anregung einer passiven Mode mit einer höheren Frequenz als die der Betriebsmode wird ermöglicht, wenn die Elektronen genug von der Betriebsmode entschleunigt werden. Im Falle drei oder mehr Moden kann Mode Locking stattfinden, wenn der Strom sehr viel höher als der Startstrom ist, auch wenn eine Mode sich im Bereich der nichtlinearen Selbstanregung befindet. Auf Grund der vorgestellten Ergebnisse kann man die Bedingungen für stabile, ein-Mode Schwingung in mehrmodigen Gyrotronen abschätzen.

PREFACE

From the earliest stages of gyrotron development, the Institute of Applied Physics at Gorky/USSR played a leading role. When KfK started development activities on advanced gyrotrons in 1983, the basic theory was well established and a considerable body of experimental results was available.

To accelerate our entry into this new field of research, it was obviously desirable to establish an exchange with the Institute at Gorky and to participate in the knowledge and experience collected there over more than 15 years. As a first step we were pleased to have had Prof. G.S. Nusinovich as a guest for two weeks at the Institut für Kernphysik II, Kernforschungszentrum Karlsruhe. During this stay, G.S. Nusinovich presented a series of lectures and kindly made available to us the manuscripts, which are comprised in this booklet.

These lectures provide a far more systematic and comprehensive treatment of mode competition and start up phenomena than is otherwise published in the literature. Thus they provide us with very useful guidelines for the development of a program package to calculate gyrotron phenomena for the KfK gyrotron experiment. During the time since they were given, we have used them as a basis for our own treatment of the problem, adapted to the parameters of our experiment.

With the agreement of the author and of the Academy of Sciences of the USSR, we are pleased to make these lectures available to the gyrotron community.

We are grateful to the Institute of Applied Physics, Academy of Sciences of the USSR for making possible the visit of Prof. Nusinovich, and we hope that this was just the beginning of a fruitful cooperation.

Minor modifications, such as the correction of obvious misprints, as well as the insertion of figure captions (to comply with guidelines for KfK publications) have been made without further correspondence with the author.

E. Borie
G. Hochschild

INDEX

| | page |
|--|------|
| Lecture 1 | 1 |
| Introduction | 1 |
| Enhancement of the generated power | 1 |
| Increase in the operating frequency | 2 |
| Extension of the microwave pulse duration | 2 |
| Mode Selection | 4 |
| Radial mode selection | 4 |
| Azimuthal mode selection | 5 |
| Equations of a Multimode Gyrotron | 7 |
| Lecture 2 | 14 |
| Stability of Single-Mode Oscillations for Purely Amplitude and Phase-Amplitude Interaction of Gyrotron Modes | 14 |
| The stability of single-mode oscillations for purely amplitude mode interaction | 16 |
| Automodulation instability | 21 |
| Lecture 3 | 27 |
| Start-Up Scenario | 27 |
| Basic Effects of Mode Interaction | 33 |
| Purely amplitude mode interaction | 34 |
| Lecture 4 | 41 |
| Phase-amplitude mode interaction | 41 |
| Space-Time Analysis of Nonstationary Processes in Multimode Gyrotrons | 47 |
| A gyrotron with a whispering gallery wave | 47 |
| A quasioptical gyrotron | 48 |
| A gyrotron with a nonfixed axial structure of the RF field | 51 |
| Conclusion | 53 |
| REFERENCES | 54 |
| FIGURE CAPTIONS | 57 |
| FIGURES | 60 |

THEORY OF MODE INTERACTION IN THE GYROTRON

G.S. Nusinovich

Institute of Applied Physics, Academy of
Sciences of the USSR, Gorky, USSR

LECTURE I

Introduction

The development of a powerful microwave electron oscillator usually takes place in three main directions:

- enhancement of the generated power,
- increase in the operating frequency,
- extension of the microwave pulse duration and/or transition to CW operation.

What is the move in each direction connected with?

Enhancement of the generated power

$$P = \eta UI \quad (1)$$

can, obviously, take place owing to an increase in the operating voltage U and the beam current I (the potentialities of increasing the electron efficiency η for highly effective microwave oscillators cannot lead to significant increase in the generated power). As the operating voltage and the beam current grow, the amplitude of stationary microwave oscillations A increases in accordance with the balance equation

$$\eta UI = \frac{\omega}{Q} A^2 V. \quad (2)$$

The left-hand part of (2) is the microwave power transferred from the electron beam to the RF field of the resonator, the right-hand part is the power of microwave losses in the resonator (V is the resonator volume, ω is the operating frequency, Q is the Q-factor of the resonator). Since quite definite values of the oscillation amplitude A and the length of the interaction space L usually correspond to high-efficiency operation, in order to maintain a constant efficiency with an increase in the power of the electron beam and microwave oscillations, it is necessary to enlarge the cross-section of the interaction space $S_{\perp} (V=S_{\perp}L)^*$.

Increase in the operating frequency for a constant level of microwave power is also needed for enlarging the resonator cross-section, because when the gyrotron operates at a fixed mode of the resonator, all sizes of the resonator diminish proportionally to the wavelength λ and the microwave power drops according to the balance equation (2). So, to keep the level of the microwave power constant, it is necessary to enlarge the resonator cross-section in the wavelength scale, i.e. to operate at higher modes of the resonator.

Extension of the microwave pulse duration and CW operation can make the resonator heating that is caused by ohmic losses of microwave power essential. The power density of the ohmic losses

* We do not discuss here the possibilities of diminishing the Q-factor, because for powerful gyrotrons the diffraction Q is usually close to the minimum value $Q \approx Q_{dif}^{min} \approx 8\pi(L/\lambda)^2$. Some comments on gyrotrons with low-Q cavities will be given below in Lecture 4.

ses is determined by the expression

$$p_{ohm} = \frac{Q_{dif}}{Q_{ohm}} \cdot \frac{P}{S_l}, \quad (3)$$

where the ohmic Q is proportional to the ratio of the resonator radius R to the skin layer depth $d \sim \lambda^{1/2}$: $Q_{ohm} \sim R/d$ and the lateral surface of the cylindrical cavity (open in the axial direction) is equal to $S_l = 2\pi RL$. Therefore if the power density of ohmic losses is too large for the mentioned gyrotron operation (for CW operation the upper limit is of order 1 kW/cm^2), in order to avoid the resonator overheating one should enlarge the resonator cross-section.

So, all the named directions of powerful gyrotron development are concerned with the tendency to space-extended systems.

It was mentioned above that the increase of the resonator cross-section leads to operation at high modes with a dense spectrum of eigenfrequencies. The distance between the frequencies of neighbouring modes is proportional to

$$\frac{\Delta\omega}{\omega} \sim \frac{\lambda^2}{S_l} \quad (4)$$

(this formula takes into account the fact that effective axial mode selection can be provided in cylindrical open resonators [1] of gyrotrons). At the same time, the gyrotron active medium that is an ensemble of electrons with the time of transition through the resonator $T = L/v_{||}$ ($v_{||}$ is the electron axial velocity), has a typical band of amplification

$$\Delta\omega_{am} \sim \frac{\pi}{T}. \quad (5)$$

Hence, when the distance between the neighbouring mode eigenfrequencies given by (4) is smaller than the active medium band (5), several modes of the gyrotron can be excited simultaneously. Un-

der such conditions the problem of providing stable single-mode oscillations with high efficiency becomes important.

Mode Selection

Before the discussion of the problem on simultaneous excitation of several modes, it should be mentioned that relation (4) is valid unless we do not use different methods of transverse mode selection.

Radial mode selection can be provided with a coaxial inner cylinder in the resonator [2]. Such a cylinder tapered to the collector pushes the rays of modes with a large radial index ρ out of the resonator, i.e. diminishes their diffraction Q . On the contrary, when the radius of the inner cylinder increases to the collector, the Q -factor of these modes becomes larger than the Q -factors of the whispering gallery modes with a large azimuthal index m ($m \gg \rho$). This can take place when the inner cylinder with the radius Υ does not significantly disturb the field of the whispering gallery modes localized near the resonator wall, i.e. when the caustic radius of these modes $R_c = \frac{m}{\nu} R$ is greater than Υ (here R is the radius of the resonator wall, $\nu = 2\pi \frac{R}{\lambda}$ is determined by the boundary condition $J'_m(\nu) = 0$ for the TE-modes).

The other method of radial mode selection can be called electron selection (in contrast to the previous one, that is electrodynamic selection). This method consists in the appropriate choice of the radius of the electron guiding center R_0 . Indeed, in gyrotrons the electron beam has a small spread in R_0 ($\Delta R_0 \ll \lambda$), which permits one to diminish the drop in electron efficiency caused by the difference in the impedance of coupling between different electrons and the resonator field.

For conventional gyrotrons with a cylindrical resonator and axially symmetric electron beam, the coupling impedance is proportional to

$$K = \frac{J_{m \pm n}^2(k_{\perp} R_0)}{(\nu^2 - m^2) J_m^2(\nu)}$$

Here k_{\perp} is the transverse wavenumber that is close to $\frac{2\pi}{\lambda}$ because gyrotrons usually operate near cutoff, n is the number of the resonant cyclotron harmonic ($\omega \approx n\omega_H$), the sum ' $m+n$ ' in the Bessel function index corresponds to the case where electrons in the external magnetic field and the electromagnetic wave in the resonator rotate in opposite azimuthal directions, ' $m-n$ ' corresponds to rotation in the same direction. It is known that the function $K(R_0)$ is maximum for R_0 close to the caustic radius R_c . In such a case modes with neighbouring frequencies and larger azimuthal indices (smaller radial indices) have $R_c > R_0$, so the coefficient K is small and the electrons interact with these fields weakly. For modes with larger radial indices, this radius of the electron guiding center R_0 corresponds to subsequent peaks of the Bessel function whose maxima are smaller than the inner one. Note, by the way, that modes with larger radial indices occupy a larger part of the resonator volume (in the expression for K this fact corresponds to a large value of $\nu^2 - m^2$ for the given ν), hence, the starting currents of these modes grow with an increase in ρ .

Azimuthal mode selection. For azimuthal mode selection it is necessary to disturb the azimuthal symmetry of the interaction space of conventional gyrotrons. The simplest way to do this is to make axial slots in the resonator [3,4]. When the distance between the two halves of such a cavity grows, this resonator

transforms to an open quasioptical two-mirror resonator [5] (gyrotrons with such quasioptical resonators have been actively investigated in recent years, see, for example, [6,7]). It is obvious that in two-mirror resonators the modes with one azimuthal variation at the mirror surface have highest diffraction Q.

Thus, the use of any method mentioned above* sets a condition for the density of competing modes that is far less rigid than (4):

$$\frac{\Delta\omega}{\omega} \sim \frac{\lambda}{L_{\perp}} \quad (6)$$

In (6) a typical transverse size L_{\perp} for modes differing in radial indices p is the resonator diameter (the difference between the eigenvalues ν for such neighbouring modes with $p \gg 1$ is close to π); for the whispering gallery modes that satisfy the condition $m\lambda = 2\pi R_c$, $L_{\perp} = 2\pi R_c$; for the modes of the quasioptical resonator that satisfy the condition $p\frac{\lambda}{2} = 2l$ ($p \gg 1$, $2l$ is the distance between the mirrors), $L_{\perp} = 4l$.

Nevertheless, as the transverse sizes of the interaction space grow, even a relatively large distance between the mode eigenfrequencies (6) can become smaller than the amplification band (5). In such a case, the self-excitation conditions can be fulfilled for several modes simultaneously. The amplitudes of these modes grow independently until they become so large that the non-linear properties of the electron beam provoke mode interaction.

* Besides the mentioned methods of mode selection, there exist other methods that consist, for example, in step-profiling of the resonator [8,9].

Equations of a Multimode Gyrotron

Every resonant microwave electron oscillator can be described by a self-consistent set of equations which consists of the equation of electron motion in the RF field and the equation of the resonator field excitation by the electron beam. It is well known (see, for example, [10,11]) that the equation of electron motion has just the same form for the gyrotron as for a nonlinear oscillator under the action of the external alternating force whose frequency is close to one of the harmonics of the oscillator eigenfrequency. When the RF field acting on electrons is a sum of several modes of the resonator, the external force is a superposition of all these modes and, correspondingly, the averaged equation of electron motion has the form [12,13]

$$\frac{da}{d\xi} - i[\Delta + |a|^2 - 1]a = i \left\{ \sum_s a^{n_s-1} F_s \cdot f_s(\xi) e^{i(\psi_s - n_s \vartheta_0)} \right\}^* \quad (7)$$

with the boundary condition $a(0) = 1$. In (7) the complex value $a = \frac{p_{\perp}}{p_{\perp 0}} \cdot \exp\{-i(\vartheta - \vartheta_0)\}$ describes the change in the energy of electron oscillations ($p_{\perp 0}$ is the initial value of the orbital momentum, $\beta_{\perp 0} = \frac{v_{\perp 0}}{c}$ is the initial orbital velocity normalized to the light velocity) and the phase of the cyclotron rotation ($p_x + ip_y = p_{\perp} e^{i\vartheta}$) $\vartheta = \theta - \omega_a t$ related to the frequency ω_a close to the initial cyclotron frequency of electrons ω_{H_0} (ω_a is the basic frequency for the averaging of eq.(7)), ϑ_0 is the electron phase at the input cross-section of the resonator. The normalized axial coordinate ξ is proportional to the axial coordinate z : $\xi = \frac{\beta_{\perp 0}^2}{2\beta_{\perp 0}} \cdot \frac{\omega_a z}{c}$, $\Delta = \frac{2}{\beta_{\perp 0}^2} \left(1 - \frac{\omega_{H_0}}{\omega_a}\right)$. The sum of the RF forces of all modes that can resonate with electrons at different cyclotron harmonics ($\omega_s \approx n_s \omega_{H_0}$) is given in the right-hand part of (7). The func-

tions $f_s(z)$ describe the axial structure of the resonator modes, F_s and ψ_s are the normalized amplitude and phase of the s-th mode, respectively, taking its transverse structure into account

$$F_s e^{i\psi_s} = 4 \frac{A_s e^{i\alpha_s}}{H_0} \beta_{\perp 0}^{n_s-4} \left(\frac{n_s^{n_s}}{2^{n_s} n_s!} \right) L_{n_s}. \quad (8)$$

Here the amplitude of the s-th mode A_s is normalized to the value of the external magnetic field H_0 , the function $L_{n_s} = \left[\frac{c}{\omega_a} \left(\frac{\partial}{\partial X} + i \frac{\partial}{\partial Y} \right) \right]^{n_s} \Psi_s(X, Y)$ describes [10,11] the transverse structure of the s-mode Lorentz force acting on the electron with the coordinates X, Y of the guiding center, the membrane function $\Psi_s(X, Y)$ is the solution of the Helmholtz equation $\Delta_{\perp} \Psi_s + k_{\perp}^2 \Psi_s = 0$ with the boundary condition $\frac{\partial \Psi_s}{\partial n} = 0$ for the TE-modes at the resonator wall.

Equations of several mode excitation have been known for such a long time that it is difficult to establish their author now. For radio oscillators, Van-der-Pol seems to be the first to obtain these equations [14] (later they were analysed in detail for the case of two modes in papers [15,16] and elsewhere). Similar equations for optical masers were obtained by W. Lamb [17]. Finally, for microwave electron oscillators they were derived by L.A. Vainstein [18,19]. The method of their derivation is rather simple. The RF field of the resonator is presented as a sum of high-Q modes with a fixed space structure and amplitudes $A_s(t)$ that can slowly vary in time. The substitution of the RF field in such a form into the Maxwell equations with the condition $\left| \frac{dA}{dt} \right| \ll \omega A$ taken into account, permits one to reduce the wave equation to the equations of excitation that are ordinary differential equations of the first order. These equations for different types of oscillators differ only in the

form of the term responsible for a concrete active medium. For gyrotrons, in particular, these equations have the form [12,13]

$$\left\{ \begin{aligned} \frac{dF_s}{dt} &= F_s \left(-\frac{n_s}{2Q_s} + \Phi_s' \right), \end{aligned} \right. \quad (9)$$

$$\left\{ \begin{aligned} \frac{d\psi_s}{dt} &= \omega_s' - n_s + \Phi_s'' \end{aligned} \right. \quad (10)$$

Here the amplitude F_s and the phase ψ_s are determined by (8), the dimensionless time t equals $t = \omega_a t$, the dimensionless eigenfrequency of the s -th mode equals $\omega_s = \frac{\omega_s}{\omega_a} = \frac{\omega_s' + i(\omega_s'/2Q_s)}{\omega_a} = \omega_s' + i \frac{n_s}{2Q_s}$, $Q_s \gg 1$ is the Q -factor of the s -th mode, the value Φ_s called below the factor of excitation equals

$$\Phi_s = -i \int_{S_1} \left[\int \frac{I_s}{F_s} W(\vec{R}_{10}, \vec{\beta}_0) d\vec{\beta}_0 \cdot \frac{1}{2\pi} \int_0^{2\pi} \left(\int_{\zeta_s^{\text{in}}}^{\zeta_s^{\text{out}}} (a^*)^{n_s} f_s^*(z) e^{-i(\psi_s - n_s \theta_0)} dz \right) d\theta_0 \right] dS_1 \quad (11)$$

The dimensionless function $W(\vec{R}_{10}, \vec{\beta}_0)$ normalized to unity describes the electron distribution in the electron initial velocities and coordinates of the guiding centers $\vec{R}_{10} = (X, Y) = (R_0, \varphi)$, the parameter I_s is proportional to the beam current I :

$$I_s = \frac{eI}{mc^3} \cdot \frac{n_s \lambda_s^3}{2\pi^3 N_s} \left(\frac{n_s^{n_s+1}}{2^{n_s} \cdot n_s!} \right)^2 \beta_{10}^{2(n_s-3)} |L_{n_s}|^2, \quad (12)$$

N_s in (12) is the norm of the s -th mode oscillations. For a hollow annular electron beam, where the spread in electron velocities and radial coordinates of the guiding centers can be neglected,

$W(\vec{R}_{10}, \vec{\beta}_0) = \frac{1}{2\pi R_0} \delta(R_{\perp} - R_{10}) \cdot \delta(\beta_{\perp} - \beta_{10}) \cdot \delta(\beta_{\parallel} - \beta_{10})$ and, thus, $\Phi_s = I_s \hat{\Phi}_s$, where

$$\hat{\Phi}_s = -\frac{i}{F_s} \cdot \frac{1}{2\pi} \int_0^{2\pi} \left\{ \frac{1}{2\pi} \int_0^{2\pi} \left[\int_{\zeta_s^{\text{in}}}^{\zeta_s^{\text{out}}} a^{*n_s} f_s^*(z) e^{-i(\psi_s - n_s \theta_0)} dz \right] d\theta_0 \right\} d\varphi, \quad (11a)$$

Comparing equations (9) with the known equations of excitation (see, for example, [10,7]), where the active medium is described

by the polarization $\vec{P} = \chi \vec{E}$ (χ is the dielectric susceptibility), one can easily relate Φ and χ : $i\Phi = \frac{1}{2}\chi$.

In view of the assertion that eqs.(9) and (10) are ordinary differential equations of the first order, it is necessary to note that, in principle, the factor of excitation Φ_s (11) is determined as the integral over the resonator volume at a given moment of time t . At this moment the electrons which interacted with the RF field at a time $t - t'$, where $0 \leq t' \leq T = \frac{L}{v_{||}}$, are present in the resonator volume. Hence, the gyrotron active medium, similar to active media of other microwave electron devices, possesses space-time dispersion and eqs.(9) and (10) are integro-differential equations with a delay argument.

The processes in the multimode gyrotron described by eqs.(7), (9) and (10) can be characterized by some typical times. For electrons, this is the transit time $T = \frac{L}{v_{||}}$ during which an electron passes through the resonator. This time determines the typical width of the Lorentz force spectrum and, correspondingly, the band of amplification (5). The typical time for mode amplitudes in a "cold" resonator is the time of the oscillation decay $\tau_d \sim Q_s / \omega_s$. For a resonator filled by electrons, the typical time for nonstationary processes is the time of the amplitude growth which, as follows from eq.(9), is proportional to $\tau \sim \frac{I_{st}}{I - I_{st}} \cdot \frac{Q_s}{\omega_s}$. Since under usual conditions the beam current I exceeds the starting value I_{st} only by several times, one can consider τ to be of the order of τ_d . The beating effects play an important role for phase relations between the modes. These effects depend on the distance between the mode frequencies: for two modes, $\tau_b \sim |\omega_1 - \omega_2|^{-1}$; for three modes, besides $\tau_b \sim |\omega_i - \omega_j|^{-1}$ ($i, j = 1, 2, 3; i \neq j$), such times as $\tau_b \sim |\omega_i + \omega_j - 2\omega_k|^{-1}$ ($i, j, k = 1, 2, 3; i \neq j \neq k$)

can be essential and so on. Note, that for gyrotrons with the axial symmetry of the interaction space $\Psi_s = J_{m_s}(k_s R) e^{-im_s \varphi}$ and, as follows from (8), $L_{n_s} = J_{m_s \pm n_s}(k_s R_0) e^{-i(m_s \pm n_s) \varphi}$, the phase Ψ_s is a sum of the term α_s depending on time and the term $(m_s \pm n_s) \varphi$ depending on the azimuthal coordinate φ : $\Psi_s = \alpha_s - (m_s \pm n_s) \varphi$. Therefore, the beating harmonics in eqs.(9) and (10) have the form $(\omega_2 - \omega_1)t - (m_2 - m_1)\varphi$, $(2\omega_2 - \omega_1 - \omega_3)t - (2m_2 - m_1 - m_3)\varphi$ and so on.

Taking into account the expression for diffraction Q $Q_{diff}^{min} \approx 8\pi (L/\lambda)^2$ given above, one can determine the ratio of both times $\tau/T \approx [I_{st}/(I - I_{st})] \cdot 4\beta_{||} (L/\lambda)$. Since under typical conditions in gyrotrons $4\beta_{||} \cdot I_{st}/(I - I_{st}) \sim 1$ and $L \gg \lambda$, the time of the mode amplitude growth is much greater than the electron transit time T . This fact permits one to integrate the equation of electron motion (7) assuming the mode amplitudes to be constant and, then to analyse "slow" evolution of the mode amplitudes, i.e. eqs.(9).

The typical times of phase beatings, in the general case, can be comparable with the electron transit time T because the distance between the mode eigenfrequencies can be of the order of the amplification band. Correspondingly, the equation of electron motion (7) should be integrated for different values of phase differences $\Psi_2 - \Psi_1$, $2\Psi_2 - \Psi_1 - \Psi_3$ and so on, which increases the time of computer analysis significantly. At the same time, in many cases the equations for mode amplitudes (9) do not depend on the phase differences $\Delta\Psi$. These cases are:

a) Fast beating in time. This case corresponds to a large distance between the mode eigenfrequencies $(\omega_2 - \omega_1)$, $(2\omega_2 - \omega_1 - \omega_3)$ and so on, as compared with the width of the mode resonant curve ω_s/Q_s .

b) Azimuthal orthogonality of modes with different azimuthal

indices when $m_1 \neq m_2$, $2m_2 \neq m_1 + m_3$ and so on.

In the first case, one can average eq.(9) over the time scale $\sim Q_s/\omega_s$ and thus exclude all fast oscillations of different phases. In the second case, the phase differences vary with the azimuthal coordinate φ and, hence, the integration over φ in the expression for the factor of excitation (11) will lead to the averaging over the phase beating in eqs.(9) and (10). Since in such cases eq.(9) for mode amplitudes does not depend on mode phases, purely amplitude interaction takes place between the modes, i.e. one mode amplitude evolution is affected only by the amplitudes of other modes, not by their phases.

On the contrary, when several modes with a quasiequidistant spectrum are in the cyclotron band and relations such as $2m_2 = m_1 + m_3$ can be valid for the azimuthal indices of these modes, the amplitude evolution of these modes depends not only on the mode amplitudes, but on their different phases as well. Whisperring gallery modes in a resonator with a large radius can be an example of such a case. The condition $2m_2 = m_1 + m_3$ is valid for azimuthal indices of these modes that differ only by a unity. The spectrum of these modes is close to an equidistant one: representing the eigenvalues $\nu_{m,p}$ for large m in the form [5] $\nu_{m,p} = m - t_p \left(\frac{m}{2}\right)^{1/3}$ (t_p is the p -th root of the equation $U'(t) = 0$, U is the Airy function), one can obtain the estimation [20] $\frac{|\omega_1 + \omega_3 - 2\omega_2|}{\omega_2} \approx \frac{2}{3} |t_p| \left(\frac{m}{2}\right)^{1/3} \cdot \frac{1}{m^3}$. For $m \gg 10$ and $p \leq 3$ ($|t_1| = 1.02$, $|t_2| = 3.25$, and $|t_3| = 4.82$), this frequency difference is not greater than the width of the resonance curve for modes with $Q \sim 10^3$. So, in this case beating with the phase difference $2\psi_2 - \psi_1 - \psi_3$ will be presented in eq.(9) for the mode amplitudes and, hence, it will be ne-

cessary to analyse these equations together with the corresponding equation for phase $2\psi_2 - \psi_1 - \psi_3$.

LECTURE 2

Stability of Single-Mode Oscillations for Purely Amplitude and Phase-Amplitude Interaction of Gyrotron Modes

In this lecture we shall restrict our consideration to the investigation of the simplest and, perhaps, most important problem in a large number of problems concerning mode interaction, namely, the stability of single-mode stationary oscillations. The simplicity of this problem is explained by the fact that only the vicinity of the equilibrium state on the F-axis will be investigated in the $(2N-1)$ -coordinate space that corresponds to the enhancement of the N-modes (with N amplitudes and N-1 phase differences).

This investigation can be readily divided into two stages, the first of which is the analysis of stationary single-mode oscillations of the operating mode and the second one is the study of the stability of these oscillations with respect to the parasitic mode oscillations whose amplitudes are assumed to be small as compared to the amplitude of the operating mode.

A self-consistent set of equations for stationary single-mode oscillations in the gyrotron follows from eqs.(7), (9) and (11a):

$$\left\{ \begin{array}{l} \frac{da_{(j)}}{dt} - i(\Delta + |a_{(j)}|^2 - 1)a_{(j)} = iF_0 f_0^*(\xi) (a_{(j)}^*)^{n_0-1}, \end{array} \right. \quad (13)$$

$$\left\{ \begin{array}{l} \Phi_0 = -i \frac{I_0}{F_0} \cdot \frac{1}{2\pi} \int_0^{2\pi} \left\{ \int_0^{\xi_{out}} (a_{(j)}^*)^{n_0} f_0^*(\xi) d\xi \right\} d\vartheta_0, \end{array} \right. \quad (14)$$

$$\left\{ \begin{array}{l} \Phi_0' = \frac{n_0}{2Q_0}. \end{array} \right. \quad (15)$$

The boundary condition for (13) is just the same as for (7):

$a_{10}(0) = 1$. The index "0" here corresponds to the operating mode and its action on the electrons, the frequency ω_a in this lecture is equal to ω_0 . Equation (15) corresponds to the balance equation (2) given below in the dimensional variables.

The set of equations (13)-(15) was analysed in many papers concerned with the theory of single-mode oscillations in the gyrotron (see, for example, [10]). These equations permit one to determine the amplitude of the operating mode F_0 for the given values of the beam current parameter $I_c Q_0$, the cyclotron resonance mismatch Δ and the axial structure of the resonator RF field $f_0(z)$. The results of numerous investigations of these equations are summarized elsewhere (see, for example, [10, 21] and [22]).

In the study of the stability of these oscillations we shall distinguish two possible cases that were discussed in the first lecture: the case of purely amplitude interaction and the case of phase-amplitude mode interaction. In the first case, it suffices to analyse the stability of the operating mode oscillations with respect to one, arbitrary, parasitic mode, since parasitic modes do not affect one another in this case and the condition of their self-excitation depends only on the intensity of the operating mode. On the contrary, in the case of phase-amplitude mode interaction, where the conditions of time

$(|2\omega_0 - \omega_{-1} - \omega_{+1}| \leq \frac{\omega}{Q})$ and space $(2m_0 = m_{-1} + m_{+1})$ synchronisms are satisfied, the parasitic modes are coupled. Here, when the single-mode oscillations of the operating mode become unstable, the oscillations of both satellites appear simultaneously. This fact can be interpreted as automodulation of the operating mode oscillations and, hence, this instability can be called automodulation instability.

The stability of single-mode oscillations for purely amplitude mode interaction [13,23]

Let us suppose that parasitic mode oscillations with a small amplitude $F_1 \ll F_0$ appear in the gyrotron with intense oscillations of the operating mode. This fact will provoke small perturbations in the electron motion. We shall describe these perturbations assuming the value a to be equal to $a_{(0)} + F_1 a_{(1)}$. Linearizing eq.(7) in F_1 , we obtain the equation for $a_{(1)}$ from (7) and (13):

$$\frac{da_{(1)}}{dz} - i(\Delta + 2|a_{(0)}|^2 - 1)a_{(1)} - ia_{(0)}^2 a_{(1)}^* = i \left\{ (n_0 - 1) a_{(0)}^{n_0 - 2} \int_0 F_0 a_{(1)} + a_{(0)}^{n_1 - 1} \int_1 e^{i(\tilde{\Delta}z + \psi)} \right\}^* \quad (16)$$

This equation should be supplemented with a complex-conjugate equation for $a_{(1)}^*$ and the boundary condition $a_{(1)}(0) = 0$. The phase ψ denotes here the difference $\psi = (n_0 \omega_1' - n_1 \omega_0') t_0 + (n_1 m_0 - n_0 m_1) \varphi$ of phases of both modes at the moment t_0 when the electrons enter the input cross-section at the point with the azimuthal coordinate φ . The value $\tilde{\Delta}$ equals $\tilde{\Delta} = \frac{2}{\beta_{10}^2} \left(\frac{\omega_1'}{\omega_0'} - \frac{n_1}{n_0} \right)$. The expression for the factor of parasitic mode excitation by a hollow electron beam follows from (11a)

$$\hat{\Phi}_1 = -in_1 \cdot \frac{1}{2\pi} \int_0^{2\pi} \left\{ \frac{1}{2\pi} \int_0^{2\pi} \left[\int_{\Sigma_1^{in}}^{\Sigma_1^{out}} (a_{(0)}^{n_1 - 1} \cdot a_{(1)} \cdot f_1)^* e^{-i(\tilde{\Delta}z + \psi)} dz_1 \right] d\varphi_0 \right\} d\varphi \quad (17)$$

In view of the fact that we consider the case $n_1 m_0 \neq n_0 m_1$ the averaging over the azimuthal coordinate φ is identical here to the averaging over the phase difference ψ .

Using eq.(9), one can easily obtain the conditions of stability for the given equilibrium state

$$\left. \frac{\partial \Phi_0'}{\partial F_0} \right|_{F_0^{eq}} < 0, \quad \Phi_1'(F_0^{eq}) < \frac{n_1}{2Q_1}$$

The first of these conditions defines the stability of oscillations of the operating mode with a stationary amplitude with respect to its own perturbations. This condition is not fulfilled for the unstable branch of the oscillator with hard self-excitation, it is valid in the below consideration.

If the second condition is violated, the parasitic mode has a positive increment and, hence, its oscillations will grow. Taking the balance equation (15) into account, this condition can be written in the form

$$\Phi_0' / \Phi_1' > q = \frac{n_0}{n_1} \cdot \frac{Q_1}{Q_0}, \quad (18)$$

or, for the gyrotron in which the spread in electron velocities and radii of guiding centers can be neglected, in the form

$$\hat{\Phi}_0' / \hat{\Phi}_1' > \hat{q} = \frac{n_0}{n_1} \cdot \frac{I_1 Q_1}{I_0 Q_0}. \quad (18a)$$

Two facts should be emphasized. First, both factors, Φ_0 and Φ_1 , depend on the amplitude of the operating mode (for a parasitic mode, it follows from eq.(16) that determines the value $Q_{(1)}$ and, correspondingly, the factor Φ_1 , and includes the value $Q_{(0)}$ depending on F_0). Second, the given set of equations can be applied to the analysis of the competition of modes resonant with different cyclotron harmonics. A mode resonant with the lower harmonic or a mode resonant with the higher one can have some advantages in this competition depending on the beam voltage and the pitch-factor of electrons $\beta_{\perp} / \beta_{\parallel}$. Here we mean the ratio $I_1 Q_1 / I_0 Q_0$. On the one hand, the ratio of the effective impedances of coupling is proportional to the electron orbital velocity to the power that corresponds to multipole interaction of electrons with the RF field at different harmonics [11] (see (12)): $I_1 / I_0 \sim \beta_{\perp 1}^{2n_1} / \beta_{\perp 0}^{2n_0}$. On the other

hand, the diffraction Q of the resonator with a fixed length is larger for the modes resonant with higher harmonics because the wavelength is smaller, i.e. $Q_1/Q_0 \sim \frac{(L/\lambda_1)^2}{(L/\lambda_0)^2} = \frac{n_1^2}{n_0^2}$ and, thus, the ratio $I_1 Q_1 / I_0 Q_0$ is proportional to $(n_1 \beta_{10}^{n_1} / n_0 \beta_{10}^{n_0})^2$.

The integration of eq.(16) and the computation of the factor of excitation (17) can be simplified by introducing the integral variables that are independent of the phase difference ψ . Introducing the matrix

$$Y = \begin{pmatrix} Y_1 \\ Y_2 \\ Y_3 \\ Y_4 \end{pmatrix} = \frac{1}{2\pi} \int_0^{2\pi} \begin{pmatrix} a_{(1)}' \sin \xi \\ a_{(1)}'' \cos \xi \\ a_{(1)}' \cos \xi \\ a_{(1)}'' \sin \xi \end{pmatrix} d\xi,$$

where $\xi = \tilde{\Delta} \zeta + \psi$, $a_{(1)} = a_{(1)}' - i a_{(1)}''$, one can transform eq.(16) to the equation that does not include the phase ψ and has a matrix form

$$\frac{dY}{d\zeta} = G Y - H \quad (16a)$$

with the boundary condition $Y(0) = 0$. The matrix G is equal to

$$G = \begin{pmatrix} 2x \cdot y & 0 & \tilde{\Delta} & \Delta + x^2 + 3y^2 - 1 \\ 0 & -2x \cdot y & -(\Delta + 3x^2 + y^2 - 1) & -\tilde{\Delta} \\ -\tilde{\Delta} & \Delta + x^2 + 3y^2 - 1 & 2x \cdot y & 0 \\ -(\Delta + 3x^2 + y^2 - 1) & \tilde{\Delta} & 0 & -2x \cdot y \end{pmatrix},$$

where $a_{(0)} = x - iy$, and the matrix H for the modes resonant with the fundamental cyclotron harmonics is

$$H = \begin{pmatrix} -\frac{1}{2} f_1 \\ \frac{1}{2} f_1 \\ 0 \\ 0 \end{pmatrix}$$

Hence, the factor Φ can be determined by the expression that follows from (17):

$$\hat{\Phi}_1 = -i \frac{1}{2\pi} \int_0^{2\pi} \left[\int_{\zeta_1^{in}}^{\zeta_1^{out}} (\Upsilon_1 - \Upsilon_2) f_1^*(\zeta) d\zeta \right] d\nu_0 \quad (17a)$$

and does not include the phase ψ . The expressions for H and $\hat{\Phi}_1$ for the case of higher cyclotron resonances are given in [23].

Thus we have reduced our study to the following procedure. In the first stage, we integrate the equation of electron motion in the field of the operating mode (13) and determine $a_{(o)}(\zeta)$. Then, we calculate the factor Φ_0 (14) and find from the balance equation (15) the value of the beam current parameter $I_0 Q_0$ that corresponds to the given amplitude of the operating mode F_0 . In the second stage, we determine the perturbation in the electron motion $a_{(p)}(\zeta)$ that is caused by the field of the parasitic mode using eq. (16a) and calculate the factor Φ_1 (17a). After all these calculations we can determine the highest value of \hat{Q} for which the condition of operating mode stability (18a) is valid.

The results of the calculations were given in [23, 13]. As an example, the dependence of the real part of the factor of parasitic mode excitation Φ_1 on the frequency mismatch $\Delta_1 =$

$$= \Delta_o + \tilde{\Delta} = \frac{2}{\beta_{1o}^2} \cdot \frac{\omega_1 - \omega_{H_o}}{\omega_o} \quad (n_{o,1} = 1) \quad \text{is given in Fig.1 [13]}$$

for the gyrotron in the absence of the operating mode oscillations ($\hat{\Phi}'_{1,L}$) and in the presence of these oscillations with

the amplitudes $F_o = 0.04$ and different values of mismatch

$$\Delta_o = \frac{2}{\beta_{1o}^2} \cdot \frac{\omega_o - \omega_{H_o}}{\omega_o} \quad (\text{the corresponding values of } \hat{\Phi}'_o \text{ are shown in Fig.1 by horizontal dashed lines, } f_{o,1}(\xi) = \exp\left\{-\left(\frac{2\xi}{\xi_{out}} - 1\right)^2\right\},$$

$\xi_{out} = 17$). It follows from Fig.1 that the main effect of the operating mode is the suppression of the parasitic mode, i.e. the factor $\hat{\Phi}'_1$ in the presence of the operating mode is, as a whole, much lower than for the unexcited gyrotron. The origin of the latter effect will be analysed in the next lecture.

A most typical situation for gyrotrons is the case when the beam current is fixed and the external magnetic field is tuned for the maximum of efficiency. The corresponding dependence of the operating mode amplitude on the mismatch Δ_o for the value of the beam current parameter $\hat{I}_o = I_o \cdot Q_o \cdot \xi_{out}^4 = 10^3$ is given in Fig.2. Using such dependences for the determination of F_o as a function of Δ_o at a given value of \hat{I}_o , one can find the zone of parasitic mode self-excitation in the plane of mismatches $\Delta_o, \tilde{\Delta}$. This zone is shown in Fig.3 for the values $\hat{Q}_1 = 1$, $\hat{I}_o = 10^3$, and $\xi_{out} = 17$. It follows from Fig.3 that self-excitation of the parasitic mode can take place in the left-hand side of the zone of the operating mode oscillations where the amplitude of the operating mode is small (see Fig.2) and the parasitic mode can be enhanced with a larger amplitude if its frequency is closer to the center of the zone of self-excitation ($\tilde{\Delta} > 0$).

It should be noted that for the optimum parameters of the electron efficiency of the operating mode ($\hat{I}_o = 10^3$, $\xi_{out} = 17$, and $\Delta_o = 0.4$), the parasitic mode can be excited only when its

frequency is closer to the center of the self-excitation zone and its product of the Q-factor and the coupling impedance is twice as great as for the operating mode. The threshold curve Q_{th}^{-1} is shown in Fig.4. The oscillations of the operating mode with the maximum efficiency are unstable below this curve.

Automodulation instability [24,25]

Let us consider the problem of stability of single-mode oscillations in the gyrotron with phase-amplitude mode interaction. Due to the phase coupling, high- and low-frequency satellites can appear in such a device simultaneously. We shall assume that weak oscillations of the satellites cause small perturbation in the electron motion $a = a_{(0)} + a_{(1)}$ ($|a_{(1)}| \ll |a_{(0)}|$). The corresponding equation for $a_{(1)}$ follows from eqs.(7) and (13) and for the cyclotron resonance at the fundamental harmonic has the form

$$\frac{da_{(1)}}{d\tau} - i \left\{ [\Delta + 2|a_{(0)}|^2 - 1] a_{(1)} + a_{(0)}^2 a_{(1)}^* \right\} = i \left\{ \int_{-1}^1 F_{-1} e^{-i\bar{\Psi}_{-1}} + \int_1^1 F_1 e^{-i\bar{\Psi}_1} \right\} \quad (19)$$

Here the phases $\bar{\Psi}_{\pm 1}$ are taken with respect to the phase of the central mode $\bar{\Psi}_{\pm 1} = (\omega_{\pm 1} - \omega_0) \tau \pm \varphi + \alpha_{\pm 1} - \alpha_0$, $\tau = \frac{z}{v_{||}}$ ($0 \leq \tau \leq T$). Equation (19) similar to eq.(16) should be supplemented with a complex-conjugate equation for $a_{(1)}^*$ and a boundary condition $a_{(1)}(0) = 0$.

Similarly to the previous case, these equations can be reduced to the form that does not contain the amplitudes of parasitic modes and the azimuthal coordinate φ , introducing new variables $u_{\pm 1}$ and $U_{\pm 1}$ instead of $a_{(1)}$:

$$\begin{cases} F_1 u_1 + F_{-1} e^{i\bar{\Psi}} u_{-1} = e^{i\tilde{\Delta}\tau} \cdot \frac{1}{2\pi} \int_0^{2\pi} a_{(1)} e^{-i\varphi} d\varphi, \\ F_1 U_1 + F_{-1} e^{i\bar{\Psi}} U_{-1} = e^{i\tilde{\Delta}\tau} \cdot \frac{1}{2\pi} \int_0^{2\pi} a_{(1)}^* e^{-i\varphi} d\varphi. \end{cases}$$

Here $\tilde{\Delta} = \frac{2}{\beta_{10}^2} \cdot \frac{\omega_1 - \omega_0}{\omega_0}$, the phase $\bar{\Psi} = \bar{\Psi}_{-1} + \bar{\Psi}_{+1} = (\omega_1 + \omega_{-1} - 2\omega_0)\tau + \alpha_1 + \alpha_{-1} - 2\alpha_0$ corresponds to four-photon decay of two quanta of the operating mode to the quanta of both satellites. Equations for $u_{\pm 1}, v_{\pm 1}$ follow from eq.(19) and its complex-conjugate one:

$$\begin{cases} \frac{du_1}{d\tau} - i(\Delta_0 + \tilde{\Delta} + 2|a_{(0)}|^2 - 1)u_1 - ia_{(0)}^2 v_1 = if_1^*, \\ \frac{dv_1}{d\tau} + i(\Delta_0 - \tilde{\Delta} + 2|a_{(0)}|^2 - 1)v_1 + ia_{(0)}^{*2} u_1 = 0, \end{cases} \quad (20)$$

$$\begin{cases} \frac{du_{-1}}{d\tau} - i(\Delta_0 + \tilde{\Delta} + 2|a_{(0)}|^2 - 1)u_{-1} - ia_{(0)}^2 v_{-1} = 0, \\ \frac{dv_{-1}}{d\tau} + i(\Delta_0 - \tilde{\Delta} + 2|a_{(0)}|^2 - 1)v_{-1} + ia_{(0)}^{*2} u_{-1} = -if_{-1}^*. \end{cases} \quad (21)$$

The corresponding boundary conditions are $u_{\pm 1}(0) = 0, v_{\pm 1}(0) = 0$. Equations (20) and (21) do not include the satellite amplitudes, the azimuthal coordinate φ , and the phase difference $\bar{\Psi}$. The expression for the factor of excitation $\hat{\Phi}_{\pm 1}$ (17) can be transformed in a similar manner

$$F_1 \hat{\Phi}_1 = F_1 \Phi_{1,1} + F_{-1} e^{i\bar{\Psi}} \Phi_{1,-1}, \quad F_{-1} \hat{\Phi}_{-1} = F_1 \Phi_{-1,1} + F_{-1} e^{i\bar{\Psi}} \Phi_{-1,-1}, \quad (22)$$

where

$$\Phi_{1,\pm 1} = -i \int_0^{\tau_{out}} \left\{ \frac{1}{2\pi} \int_0^{2\pi} u_{\pm 1}^* d\varphi_0 \right\} f_{\pm 1}^*(\xi) d\xi, \quad \Phi_{-1,\pm 1} = -i \int_0^{\tau_{out}} \left\{ \frac{1}{2\pi} \int_0^{2\pi} v_{\pm 1}^* d\varphi_0 \right\} f_{-1}(\xi) d\xi \quad (23)$$

The equation for the phase difference $\bar{\Psi}$ follows from eqs.(10)

$$\frac{d\bar{\Psi}}{dt} = \frac{\omega_1 + \omega_{-1} - 2\omega_0}{\omega_0} + I_{-1} \hat{\Phi}_{-1}'' + I_1 \hat{\Phi}_1'' - 2I_0 \hat{\Phi}_0'' \quad (24)$$

If the beam current parameters for all modes and their axial structures are the same, $I_{\pm 1} = I_0$, $f_{\pm 1}(\xi) = f_0(\xi)$, and both the satellites have equal Q-factors $Q_{-1} = Q_1$, using eq.(24) and expressions (22) and (23) one can determine the stationary value of the phase $\bar{\Psi}$ (for $F_{\pm 1} \rightarrow 0$) that is stable

with respect to the phase variations

$$\cos \bar{\Psi}_{st} = \frac{1}{b^2 + c^2} \left[-c\delta - b\sqrt{b^2 + c^2 - \delta^2} \right], \quad (25)$$

$$\sin \bar{\Psi}_{st} = \frac{1}{b^2 + c^2} \left[b\delta - c\sqrt{b^2 + c^2 - \delta^2} \right].$$

Here $b = \Phi'_{1,-1} - \Phi'_{-1,1}$, $c = \Phi''_{1,-1} + \Phi''_{-1,1}$, $\delta = \frac{\omega_1 + \omega_{-1} - 2\omega_0}{I_0 \omega_0} + \Phi''_{1,1} + \Phi''_{-1,-1} - 2\hat{\Phi}_1$ is the frequency mismatch that characterizes the nonequidistance of the mode eigenfrequency spectrum (see Lecture 1) with the electron detuning of normal frequencies taken into account.

The equations for the satellite amplitudes which follow from eqs.(9) and expressions (22) for the case of phase-amplitude mode interaction are coupled:

$$\begin{cases} \frac{dF_1}{d\tau} = F_1 \left(\Phi'_{1,1} - \frac{1}{2I_0 Q_1} \right) + F_{-1} \left(\Phi'_{1,-1} \cos \bar{\Psi}_{st} - \Phi''_{1,-1} \sin \bar{\Psi}_{st} \right), \\ \frac{dF_{-1}}{d\tau} = F_{-1} \left(\Phi'_{-1,-1} - \frac{1}{2I_0 Q_1} \right) + F_1 \left(\Phi'_{-1,1} \cos \bar{\Psi}_{st} + \Phi''_{-1,1} \sin \bar{\Psi}_{st} \right), \end{cases}$$

here $\tau = I_0 \omega_0 t$. Two conditions of the operating mode stability with respect to the satellites follow from these equations

$$\sigma_1 + \sigma_{-1} < 0, \quad (26)$$

$$\begin{aligned} \sigma_1 \cdot \sigma_{-1} - \Phi'_{1,-1} \cdot \Phi'_{-1,1} \cdot \cos^2 \bar{\Psi}_{st} + \Phi''_{1,-1} \cdot \Phi''_{-1,1} \cdot \sin^2 \bar{\Psi}_{st} + \\ + \sin \bar{\Psi}_{st} \cdot \cos \bar{\Psi}_{st} \left(\Phi''_{1,-1} \cdot \Phi'_{-1,1} - \Phi'_{1,-1} \cdot \Phi''_{-1,1} \right) > 0, \end{aligned} \quad (27)$$

where $\sigma_1 = \Phi'_{1,1} - \frac{1}{2I_0 Q_1}$, $\sigma_{-1} = \Phi'_{-1,-1} - \frac{1}{2I_0 Q_1}$ are the increments of the satellites.

Thus in comparison with the case of purely amplitude mode interaction analysed above, these equations contain only one additional parameter, namely, the mismatch δ that characterizes weak nonequidistance of the mode eigenfrequency spectrum. Similarly to the previous case, only the situation where the Q-factors of all modes are equal should be analysed numerically and the case $Q_{\pm 1} \neq Q_0$ can be analysed analytically be-

cause conditions (26) and (27) can be rewritten in the form

$$\mathcal{F}_1 = \mathcal{F}_1^{(1)} + 2(1-r) \hat{\Phi}'_0 < 0,$$

$$\mathcal{F}_2 = \mathcal{F}_2^{(1)} + (1-r) \hat{\Phi}'_0 [\mathcal{F}_1^{(1)} + (1-r) \hat{\Phi}'_0] > 0,$$

where the functions $\mathcal{F}_{1,2}$ denote the expressions in the left-hand parts of conditions (26) and (27), respectively, the index (1) symbolizes the case $r = Q_0/Q_{\pm 1} = 1$.

The results of numerical investigations are given in Fig.5. The axial structure of all modes was taken in the form $f(\xi) = \exp\left\{-\left(\frac{2\xi}{\xi_{out}} - 1\right)^2\right\}$, $\xi_{out} = 10$. The solid line shows the zone of the operating mode self-excitation. The dashed line shows the beam current parameter $I'_0 = 2I_0Q_0$ optimum for the electron efficiency of the operating mode (the circle in this line corresponds to the maximum of the electron orbital efficiency). The dot-dash line corresponds to the break in the operating mode oscillations at the edge of the zone of hard self-excitation. For different values of the distance between the mode frequencies $\tilde{\Delta}$, the boundaries of the zone of the operating mode oscillation stability are given in Fig.5 for $\delta = 0$, $\hat{q} = 1$. The dashed lines correspond to condition (26) and the solid lines, to condition (27). These lines are shaded as viewed from the automodulation instability. As the distance between the mode frequencies grows, the zones of automodulation first expand (cf. the curves for $\tilde{\Delta} = 0, 0.1$ and 0.3). This fact can be explained by the growing influence of the dispersion in the gyrotron nonlinearity. Then, as the satellite frequencies move out of the amplification zone, the region of automodulation instability diminishes ($\tilde{\Delta} = 0.5$). The analyses of the cases $\frac{\omega_1 + \omega_{-1} - 2\omega_0}{I_0\omega_0} = 0.02$ and 0.05 show that weak nonequidistance of the mode eigenfrequency spectrum does not, practically, affect the boundary

of the zone of automodulation instability.

If the frequency mismatch of the cyclotron resonance for the operating mode is optimum for efficiency ($\Delta_0 = 0.6$), the dependence of the critical beam current that corresponds to the appearance of automodulation on the distance between the mode frequencies $\tilde{\Delta}$ has the form shown in Fig.6. The dashed non-shaded lines correspond to the case when the Q-factor of the operating mode is two times smaller than that of the satellites ($\hat{Q} = 2$). Even in this case, the central mode oscillations are stable for an arbitrary distance between the mode frequencies up to the beam currents exceeding the optimum one by two times and greater. The minimum value of the critical beam current parameter corresponds to the mode frequency mismatch $\tilde{\Delta}_{cr} \approx 0.3$ (see Fig.6). As the resonator radius grows and the mode frequency spectrum becomes more dense, the most "dangerous" satellites are, obviously, the ones with the frequency mismatch close to $\tilde{\Delta}_{cr}$ rather than the neighbouring satellites. It is natural to suppose that the automodulation instability is inherent in the decay processes, i.e. with an increase in the beam current after the appearance of the first pair of satellites subsequent pairs of satellites will be excited.

Thus, the results obtained demonstrate the possibility to provide stable single-mode oscillations with a high electron efficiency in gyrotrons with an arbitrary dense spectrum of the competing modes differing in their transverse structure. The types of instability analysed here can play an important role in the cases when the beam current is increased over its value optimum for efficiency in an effort to enhance the microwave power.

This conclusion permits one to establish the fact that for

gyrotrons with the beam current that does not exceed the optimum value, the most important problem is the appropriate choice of the start-up scenario that can provide for the operating mode to be first self-excited and then to operate with high electron efficiency. We shall analyse this problem in the next lecture.

LECTURE 3

Start-Up Scenario

Taking the results obtained in the previous lecture into account, we shall assume that for the excitation of the operating mode the gyrotron should be switched on so that the self-excitation conditions are fulfilled for the operating mode prior to the others. This method of providing the operating mode oscillations was proposed in [26] and then supplemented with the analysis of a number of examples in [27].

In view of the fact that we consider a system of orthogonal modes that are not coupled in the unexcited oscillator, the condition of self-excitation can be studied for any mode neglecting the presence of all the others in the spectrum of eigenfrequencies*. The corresponding condition follows from (9)

$$I_s \hat{\Phi}'_s = \frac{n_s}{2Q_s} \quad (28)$$

Here the value $\hat{\Phi}'_s$ in the framework of a small-signal theory does not depend on the oscillation amplitude and is only the function of the cyclotron resonance mismatch $\Delta_s = \frac{2}{\beta_{10}^2} \cdot \frac{\omega_s - n_s \omega_{H0}}{\omega_{H0}}$ and the axial structure of the s-th mode $f_s(z)$ [10, 28, 29]

$$\hat{\Phi}'_s = -\frac{1}{2} \left(n_s + \frac{\partial}{\partial \Delta_s} \right) \left| \int_{\zeta_s^{in}}^{\zeta_s^{out}} f_s(\zeta) e^{i\Delta_s \zeta} d\zeta \right|^2 \quad (29)$$

The value $\left| \int_{\zeta_s^{in}}^{\zeta_s^{out}} f_s(\zeta) e^{i\Delta_s \zeta} d\zeta \right|^2$ in (29) characterizes the intensity

*

Double degeneracy is, in principle, characteristic of any non-symmetric mode, since modes with different directions of azimuthal rotation $\sim \exp\{i(\omega t \pm m\varphi)\}$ have equal frequencies in the "cold" system. This degeneracy is, however, disturbed in the presence of electrons and the modes differ in the starting currents and oscillation frequencies due to the gyrotropy of the electron beam.

of the spectrum of the RF Lorentz force acting on the electrons. The first term in the right-hand part of (29) corresponds to the "M"-type bunching of electrons that leads to cyclotron absorption ($\hat{\Phi}'_{S,M} < 0$). The second one, which is proportional to the derivative of the spectrum intensity, corresponds to the "O"-type inertial bunching of electrons. It follows from (29) that the "O"-type inertial bunching is dominant for $\zeta_{out} \gg n$ (the transit angle $\Theta_s = \Delta_s \zeta_s^{out}$ is usually of order 2π) and, hence, the real part of $\hat{\Phi}'_S$ can be positive and the gyrotron can be self-excited. The dependence of $\hat{\Phi}'_S$ on the frequency mismatch Δ_s for various axial structures of the RF field was analysed elsewhere (see, for example, [29]).

The value of the starting current can be determined using equation (28) and expression (29). Under usual experimental conditions, when the electron-optical and electrodynamic systems are given, the starting current depends on the parameters that can be varied, namely, the external magnetic field and the anode U_a and the resonator U_r voltages. One should distinguish here two types of operating regimes, pulsed and CW operation. At CW operation, one can vary all the named parameters. The tuning usually reduces to a procedure when optimum voltages are chosen for the electron-optical system and then the magnetic field is tuned first for the best self-excitation of the operating mode and after this for the operation with the maximum efficiency. Correspondingly, the zones of self-excitation and oscillations are usually shown in the plane of parameters "beam current versus magnetic field". An example of such zones is given in Fig.7 taken from [30]. Here you can see the self-excitation zones of various modes in the gyrotron that is designed for operation at the $TE_{15,1,1}$ -mode at a frequency of

100 GHz (similar maps of the gyrotron can be found, for example, in [31]). According to Fig.7, one can choose a magnetic field for the minimum starting current of the $TE_{15,1,1}$ -mode. As the beam current increases, this mode will be excited and at about 40 A will oscillate with high efficiency (the magnetic field optimum for the electron efficiency is lower than that corresponding to the minimum starting current). At pulsed operation, it seems impossible to vary the magnetic field of the superconducting solenoid during one pulse, because such solenoids have a very large inductance and a very small resistance. It is also difficult to vary the beam current \bar{I} during one pulse because the current in cathodes with a temperature-limited emission is already saturated at a rather low level of the anode voltage and then grows insignificantly. Therefore, the only way to provide an appropriate start-up scenario for pulsed gyrotrons is to choose the necessary relations between the anode and the resonator voltages at the front of the pulses.

As a rule, the duration of the pulse front under experimental conditions is significantly greater than the typical time of the amplitude growth $\sim Q_s/\omega_s$ and the electron transit time $T = L/v_{||}$. The estimates show that, for example, for the gyrotron with the operating frequency of 100 GHz, the resonator Q-factor $\sim 10^3$, the resonator length $L = 5\lambda$ and the electron axial velocity $v_{||} = 0.3 c$, the time of the amplitude growth is of the order of several nanoseconds and the electron transit time does not exceed one nanosecond. This fact permits one to consider the oscillations at the front of the voltage pulses as a quasistationary process during which the parameters that depend on the voltage vary rather slowly.

In order to determine the zones of self-excitation of various modes in the plane "anode voltage U_a versus resonator voltage U_r ", one should express the parameters Δ_s and ζ_s^{out} in expression (29) for $\hat{\Phi}_s'$ in terms of U_a and U_r

$$\Delta_s = \frac{2}{\beta_{10}^2} \cdot \frac{\omega_s - n_s \omega_{H0}}{\omega_{H0}}, \quad \zeta_s^{out} = \frac{\beta_{10}^2}{2\beta_{110}} \cdot \frac{\omega_{H0} L_s}{c}. \quad (30)$$

The orbital velocity of electrons in the gyrotron adiabatic electron gun at a small space charge density can be determined by the expression [32]

$$\beta_{10}^2 = \alpha^3 \cdot \frac{U_a^2}{d^2 \cdot H_0^2}, \quad (31)$$

where $\alpha = H_0/H_c$ is the transmagnetic factor, i.e. the ratio of the external magnetic field in the resonator region, H_0 , to the magnetic field near the cathode, H_c . Introducing a critical anode voltage U_a^{cr} that corresponds to the appearance of the anode current, when the height of the first cycle of the electron trajectory equals the distance d between the cathode and the anode, one can express the ratio $d^2 \cdot H_0^2 / \alpha^2$ in (31) in terms of U_a^{cr} [33]

$$d^2 \cdot \frac{H_0^2}{\alpha^2} = d^2 \cdot H_c^2 = 2 \frac{mc^2}{e} U_a^{cr}. \quad (32)$$

Substituting this expression into (31), we obtain

$$\beta_{10}^2 = \frac{\alpha}{2} \cdot \frac{e}{mc^2} \cdot \frac{U_a^2}{U_a^{cr}}. \quad (31a)$$

The total electron velocity can be determined by the resonator voltage

$$\beta_0^2 = 1 - \left(1 + \frac{eU_r}{mc^2}\right)^{-2}. \quad (33)$$

Using expressions (29)-(33) and the balance equation (28), we can determine the self-excitation zones of different modes in the plane " U_a versus U_r " for a gyrotron with an arbitrary axial structure of modes resonant with an arbitrary cyclotron harmonic.

For a gyrotron whose axial structure of modes can be described by a gaussian function $f(\xi) = \exp\left\{-\left(\frac{2\xi}{\xi_{out}} - 1\right)^2\right\}$, the excitation factor $\hat{\Phi}'_s$ is [34]

$$\hat{\Phi}'_s = -\frac{\pi}{8} (\xi_s^{out})^2 \left(n_s + \frac{\partial}{\partial \Delta_s}\right) \exp\left\{-\frac{(\Delta_s \xi_s^{out})^2}{8}\right\}. \quad (34)$$

As an example, the self-excitation zones of the modes resonant with the fundamental cyclotron harmonic are shown in Fig.8 (see [35]) for a gyrotron with the gaussian axial structure of the RF field. The gyrotron parameters I_o , ξ_{out} and Δ_{op} correspond here to the maximum of the electron efficiency (the voltage reaches the pulse top). The self-excitation zones are given in the plane of parameters $X = \beta_{i0}^2/2$, $Y = \beta_o^2/2$. The zone of the operating mode self-excitation is shaded. The point of the maximum efficiency, as seen from Fig.8, lies in the field of hard self-excitation (the boundary of this field, where the oscillations break, is plotted by the dot-dash line) and can be attained only if the trajectory corresponding to the electron velocity components at the pulse fronts passes across the shaded zone of the soft self-excitation of the operating mode. Figure 8a shows an example of a gyrotron with a rather large distance between the frequencies of competing modes (for the operating mode, $\Delta_{op}^{opt} = 0.4$, for a high-frequency parasitic mode, $\Delta_{hf} = 0.6$, for a low-frequency one, $\Delta_{lf} = 0.2$; the modes with equal minimum

starting currents are considered). The trajectory I shows electron velocity components for equal voltage pulses at the anode and the resonator of the tube. The trajectory II corresponds to the case where the difference between the resonator voltage and the anode voltage is constant through the pulse. It is seen from Fig.8a that the first type of voltage feeding results in initial excitation of a higher-frequency parasitic mode at the pulse front. Then, its oscillations break and the operating mode appears and oscillates with high efficiency at the pulse top. The second type of voltage feeding leads to the excitation only of the operating mode in the pulsed gyrotron.

If the frequency spectrum of the competing modes is more dense (Fig.8b), the first type voltage feeding provides initial self-excitation of a high-frequency parasitic mode whose oscillations are stable while the gyrotron is crossing the shaded zone of the operating mode self-excitation and break only in the zone of the low-frequency parasitic mode self-excitation. Thus, in such a case the low-frequency parasitic mode oscillates with low efficiency at the pulse top and the oscillations are accompanied by the high-frequency parasitic mode oscillations at the pulse fronts. The second type high-voltage feeding results in nearly simultaneous excitation of both operating and low-frequency parasitic modes in this case. In order to determine the oscillations that are established in such a gyrotron it is necessary to investigate mode interaction, which is done below.

Thus, in the latter case we have come close to the limit of this kind of mode selection. Note that for a typical value

of the squared orbital velocity $\beta_{10}^2 \approx 0.2$, the case under study corresponds to the relative distance between the competing mode eigenfrequencies equal to 1%. If the frequency spectrum is more rare, the proposed method of choosing the start-up scenario of the gyrotron seems to be rather effective for mode selection. For example, even the first type high-voltage feeding in the above-mentioned gyrotron with the $TE_{15,1,1}$ operating mode (Fig.7) can provide, as seen from Fig. 9, stable oscillations of the operating mode with high efficiency.

Basic Effects of Mode Interaction

It was elucidated above that it is very difficult to provide the excitation only of one, operating, mode in a gyrotron with a very dense spectrum of the competing mode frequencies. When such a gyrotron is switched on several modes can be excited simultaneously. Let us consider the oscillations that can be established in such a device.

In order to give a clear picture for the origin of the nonlinear effects of mode interaction, we shall resort to a polynomial approximation of the dependence of the mode excitation factor Φ_s on the intensity of the RF field, that is we shall take into account only the first nonlinear terms, which permits us to describe the saturation effects in the oscillator with soft self-excitation. The corresponding expression for $\hat{\Phi}_s$ can be obtained as a result of the integration of the equation of electron motion (7) by successive iterations in $F_\Sigma = \sum_s F_s \cdot f_s(\kappa) e^{i\psi_s}$, substitution of the iteration terms obtained, $a_\kappa \sim (F_\Sigma)^\kappa$, into the expression for Φ_s (11a) and calculation of Φ_s . The equations for the

terms a_k follow from (7) [13,36]

$$\frac{da_k}{dz} - i(a_k + a_k^*) = iF_k, \quad (35)$$

the boundary conditions are $a_k(0) = 0$ for $k \geq 1$. Here, as compared to eq.(7), the fundamental frequency ω_a is taken to be equal to the initial cyclotron frequency of electrons in the input cross-section, ω_{H_0} ; the functions F_s in the right-hand part of (35) for $k \geq 1$ contain the solutions of the lower-order (in $(F_\Sigma)^k$) equations: $F_1 = F_\Sigma^*$, $F_2 = a_1^2 + 2|a_1|^2$, $F_3 = 2(a_1 a_2 + a_1^* a_2^* + a_1 a_2^*) + a_1 |a_1|^2$ and so on. The solution of equation (35) has the form

$$a_k = i \int_0^z F_k dz' + \int_0^z \left[\int_0^{z'} (F_k^* - F_k) dz'' \right] dz'. \quad (36)$$

Below, the cases of purely amplitude and phase-amplitude mode interaction will be considered separately.

Purely amplitude mode interaction

In conformity with the discussion given in Lecture 1 we shall consider here the interaction of two modes. The substitution of the solutions of eqs.(36) into the expression for $\hat{\Phi}_s$ (11a) permits us to obtain the following expression

$$\hat{\Phi}_s = \alpha_s - \beta_s F_s^2 - \gamma_{ss'} F_{s'}^2, \quad (37)$$

where $s' \neq s$ ($s, s' = 1, 2$), the coefficient α_s describes the "linear" properties of the s-th mode, the coefficient β_s is responsible for the effect of saturation by the self-field of the s-th mode, the coefficient $\gamma_{ss'}$ describes the effects of the cross-interaction of modes. All these coefficients depend on the cyclotron resonance mismatch Δ_s and the axial structure of the s-th mode; the coefficient $\gamma_{ss'}$ also depends on the distance between the mode frequencies and on

the axial structure of the s' -th mode. The expressions for these coefficients follow from (36) and (11a)

$$\begin{aligned} \alpha_s &= i \int_0^{\zeta_{out}} U_s \hat{f}_s^* d\zeta, \\ \beta_s &= -i \int_0^{\zeta_{out}} \hat{f}_s^* \left\{ \int_0^{\zeta} \left[2U_s^* \int_0^{\zeta'} U_s^2 d\zeta'' \cdot d\zeta'' + U_s^* U_s^2 - \int_0^{\zeta'} U_s^2 U_s^* d\zeta'' \right] d\zeta' \right\} d\zeta, \quad (38) \\ \gamma_{ss'} &= -i^2 \int_0^{\zeta_{out}} \hat{f}_s^* \left\{ \int_0^{\zeta} \left[2U_{s'}^* \int_0^{\zeta'} U_s U_{s'} d\zeta'' \cdot d\zeta'' + U_{s'}^* U_s U_{s'} - \int_0^{\zeta'} U_s U_{s'} U_{s'}^* d\zeta'' \right] d\zeta' \right\} d\zeta. \end{aligned}$$

Here new variables are introduced: $\hat{f}_s = f_s(\zeta) e^{i\Delta_s \zeta}$, $U_s = \int_0^{\zeta} \hat{f}_s(\zeta') d\zeta'$, $U_{s'} = \int_0^{\zeta} U_{s'} d\zeta'$. Expressions (38) are given for the gyrotron operating at the fundamental cyclotron resonance; it is assumed that $\zeta_{out} \gg 1$, i.e. the effects of the "M"-type bunching can be neglected in comparison with the "O"-type bunching [13,36]. The real part of the coefficient α_s can be reduced after the necessary transformations to the second term in expression (29).

Since the mode interaction in this case does not depend on the phase relations between the modes, we shall describe it by the equations for the intensities of two modes $M_s = F_s^2$ that follow from (9) and (37)

$$\begin{cases} \frac{dM_1}{d\tau} = M_1 (\mathcal{G}_1 - \beta_1' M_1 - \gamma_{12}' M_2), \\ \frac{dM_2}{d\tau} = \Upsilon M_2 (\mathcal{G}_2 - \beta_2' M_2 - \gamma_{21}' M_1). \end{cases} \quad (39)$$

Here $\mathcal{G}_s = \alpha_s' - \frac{1}{2I_s Q_s}$ are the mode increments, $\tau = I_1 \omega_{H_0} t$ is the dimensionless "slow" time, $\Upsilon = I_2 / I_1$, β_s' and γ_{ss}' are the real parts of the coefficients β_s and γ_{ss}' , respectively. Equations (39) have the same form as the one obtained by W.Lamb [17] for the optical maser. According

to [17], if the condition of "strong" coupling between the modes

$$\gamma'_{12} \cdot \gamma'_{21} > \beta'_1 \cdot \beta'_2 \quad (40)$$

is fulfilled, the phase portrait of the oscillator in the plane M_1, M_2 has the form shown in Fig.10a, i.e. mode competition takes place and the oscillations of one mode will be established, depending on the initial conditions. If condition (40) is not valid, weak coupling between the modes takes place and such modes coexist. The phase portrait of such a gyrotron is shown in Fig.10b. It follows directly from expressions (38) that, if the modes have identical axial structures

($f_1(z) = f_2(z)$) and the distance between their frequencies is small as compared to the cyclotron resonance band (i.e.

$\Delta_1 \approx \Delta_2$), then the coefficients β_s and $\gamma_{ss'}$ are related as $\gamma_{ss'} = 2\beta_s$ and, hence, the condition of "strong" coupling (40) is valid. Equations (39) have, in this case, the same form as for a conventional radio oscillator that was analysed in [14-16]. The dependence of the coefficients α'_s and β'_s on the transit angle $\Theta_s = \Delta_s \cdot z_{out}$ is shown in Fig.11a for a gyrotron with a constant amplitude of the RF field along the resonator axis ($f(z) = \frac{1}{z_{out}}$, $0 \leq z \leq z_{out}$); a similar dependence of $\gamma'_{ss'}$ on Θ_s is given in Fig.11b for different values of the ratio $k = (\omega_{s'} - \omega_{H_0}) / (\omega_s - \omega_{H_0})$ that characterizes the distance between the frequencies of competing modes [13].

In accordance with the data given in Fig.11, the lines for equal values of the ratio $\Psi = \gamma'_{12} \cdot \gamma'_{21} / \beta'_1 \cdot \beta'_2$ that defines the degree of mode coupling, are plotted in Fig.12 in the plane of transit angles of both modes Θ_s and $\Theta_{s'} = \Delta_{s'} \cdot z_{out}$ [36].

One can see from Fig.12 that as the distance between the fre-

quencies of competing modes in the zone of soft self-excitation ($\beta_s' > 0$) grows, the degree of mode coupling Ψ increases. This effect can be explained by the fact that we consider a gyrotron with a negligibly small spread in the electron velocities and the radii of the guiding centers (these factors weaken the mode coupling [37]). In addition, the electrons differing in the azimuthal coordinate of the guiding centers interact with the rotating or symmetric modes of the cylindrical resonator with equal efficacy. That is why the space-extended electron beam rolled by the rotating modes of the gyrotron becomes equivalent to the elementary beam of electrons with a common guiding center and, hence, two modes excited due to the interaction with the same electrons behave similarly to two kinds of beasts feeding on the same prey, one of them suppressing the population of the other [38]. Under such conditions, the transit effects that stipulate the dispersion of the gyrotron nonlinearity play the dominant role. In particular, when one mode frequency tends to the boundary of the soft self-excitation zone and $\beta_s' \rightarrow 0$, the coefficient $\gamma_{ss'}$, as seen from Fig.11b, can be rather large owing to the cross-interaction of modes. As a result, the degree of mode coupling grows when $\beta_s' \rightarrow 0$ (see Fig.12).

Besides the mode competition analysed above, which is the basic effect of purely amplitude mode interaction, the opposite effect can take place, namely, nonlinear mode excitation [13]. The possibility of such an effect is self-evident in Fig.11b which shows that the coefficient $\gamma_{ss'}$ is negative for a rather large value of the transit angle Θ_s . In this situation, the growth of the intensity of the s' -th mode, as follows from (39), enhances the increment of the s -th mode,

i.e. even if the self-excitation condition in the unexcited gyrotron is not fulfilled for the s -th mode ($\mathfrak{G}_s < 0$), this mode can be excited owing to the appearance of the oscillations of the s' -th mode with the intensity $M_{s'} > |\mathfrak{G}_s| / |\gamma'_{ss'}|$.

This effect can be explained by the quantum theory interpretation. From this point of view, the active medium of the cyclotron resonance masers (i.e. the electron beam) has a quasiequidistant (not equidistant) spectrum of energy levels. Due to this fact the zones of positive and negative reabsorption of the coherent cyclotron radiation are located at close frequencies and, hence, the zones of mutual suppression and excitation are also neighbouring ones.

This effect can also be explained by simple kinematic speculations. For this purpose one should bear in mind that the s' -th mode affects the electrons and the newly formed electron bunch finds itself in the decelerating phase of the s -th mode and, hence, the conditions for this mode to be excited by the bunching electron beam seem to be better than in the absence of the s' -th mode.

It is shown in [13] that this effect takes place when first the mode with a low starting current is excited and then the growth of its intensity promotes the appearance of the other mode with a higher frequency. The latter one can have a negative initial increment $\mathfrak{G}_s < 0$, but if it is in the zone of hard self-excitation ($\beta'_s < 0$), it can oscillate with high efficiency. A direct numerical analysis of eqs.(7) and (9) shows that this effect takes place when the electron beam current is much larger than the value optimum for efficiency (see Fig.13 taken from [39]). This effect was evidently observed in the experiments [40] and under the gyrotron opera-

tion at the second harmonic of the cyclotron frequency [31], where as shown in [13], the oscillations at the second harmonic provoke the excitation of parasitic modes at the fundamental cyclotron resonance. Here, the reason for the nonlinear excitation of parasitic modes at the fundamental resonance lies in the fact that the modes resonant with the second harmonic have larger rates of saturation, which leads to the disturbance of the condition of their stability (see (18) in Lecture 2) as the amplitude of this mode grows [13,41].

The results obtained permit us to demonstrate an example of the evolution of the zones of self-excitation of two modes in the plane of mismatches $\Delta_1 = \frac{2}{\beta_{10}^2} \cdot \frac{\omega_1 - \omega_{H_0}}{\omega_{H_0}}$, $\tilde{\Delta} = \frac{2}{\beta_{10}^2} \cdot \frac{\omega_2 - \omega_1}{\omega_{H_0}}$ (Fig.14) [13]. Let us assume that the electron beam current was increased rapidly at a certain initial moment of time, thus providing the possibility for the gyrotron self-excitation. So long as the mode intensities in such a gyrotron are rather small, the self-excitation zones of both modes have a symmetric form (they are shown in Fig.14, where the increment of the second mode in the shaded zone is larger than that of the first mode, the axial structure of the resonator field is $f(\xi) = \exp \left\{ - \left(\frac{2\xi}{\xi_{out}} - 1 \right)^2 \right\}$, $\xi_{out} = 17$, the beam current parameter is $I_0 = I_s Q_s \xi_{out}^4 = 10^3$). If the cyclotron resonance mismatch of the first mode Δ_1 corresponds to the minimum of the starting current and the mismatch $\tilde{\Delta}$ is nonzero, the first mode has a larger increment and its oscillations grow faster. As the first mode intensity grows, the self-excitation zone of the second mode changes as shown in Fig.14 (the curve marked $F_1 \neq 0$): the first mode suppresses the oscillations of the second one at the right edge of the oscillation

zone (where the amplitude of the first mode is large) and in the region of small mismatches between the mode frequencies $\tilde{\Delta}$ (where the effects of mode competition are dominant). At the same time, at the left edge of the oscillation zone, where the conditions for the first mode are far from optimum and its amplitude is rather small, the second mode with a higher frequency that can oscillate with a larger amplitude can be self-excited and, owing to the effect of nonlinear excitation, its self-excitation zone spreads in the direction of large mismatches $\tilde{\Delta}$.

Thus, we can now answer the question that arose when we analysed the start-up scenario. When the self-excitation conditions for two modes with close eigenfrequencies are fulfilled nearly simultaneously (the separatrix with the "saddle" state of equilibrium in Fig. 10a is close to the bisectrix of the quadrant M_1, M_2), the oscillations of one of the competing modes will be established with almost equal probability depending on the initial fluctuations of the radiation in the oscillator. Note, that in such a case each of the two modes will oscillate with practically equal efficiency because these modes have equal Q-factors, coupling impedances and close frequencies.

LECTURE 4

Phase-amplitude mode interaction

In order to describe the phase-amplitude mode interaction, we should take into account three or more modes for which the conditions of time $|2\omega_2 - \omega_1 - \omega_3| \leq \frac{\omega}{Q}$ and space (azimuthal) $2m_2 = m_1 + m_3$ synchronism are fulfilled. Using the method of successive iterations in $F_\Sigma = \sum_s F_s \cdot f_s(\zeta) e^{i\psi_s}$ for the integration of the equation of electron motion and the computation of the factors of excitation, one can obtain the expressions for $\hat{\Phi}_s$ [13] similar to (37)

$$\hat{\Phi}_s = \alpha_s - \beta_s F_s^2 - \sum_{s' \neq s} \gamma_{ss'} F_{s'}^2 - \frac{\xi_s}{F_s} \begin{cases} F_2^2 F_3 e^{-i\bar{\psi}}, & s=1 \\ F_1 F_2 F_3 e^{i\bar{\psi}}, & s=2 \\ F_2^2 F_1 e^{-i\bar{\psi}}, & s=3. \end{cases} \quad (41)$$

Here $\bar{\psi} = \psi_1 + \psi_3 - 2\psi_2$ is the phase difference that corresponds to the synchronous harmonic of the alternating current. The expressions for the coefficients ξ_s that describe the phase coupling of modes, have the form [13]

$$\xi_1 = -i \int_0^{\zeta_{out}} \hat{f}_1^* \left\{ \int_0^{\zeta'} [2u_3^*] \int_0^{\zeta''} [u_2^2 d\zeta'' + u_3^* u_2^2 - \int_0^{\zeta''} u_2^2 u_3^* d\zeta''] d\zeta' \right\} d\zeta, \quad (42)$$

$$\xi_2 = -2i \int_0^{\zeta_{out}} \hat{f}_2^* \left\{ \int_0^{\zeta'} [2u_2^*] \int_0^{\zeta''} [u_1 u_3 d\zeta'' + u_2^* u_1 u_3 - \int_0^{\zeta''} u_1 u_3 u_2^* d\zeta''] d\zeta' \right\} d\zeta.$$

The expression for ξ_3 follows from the expression for ξ_1 , provided that we change the indices $1 \rightleftharpoons 3$. All variables in (42) are just the same as in formula (38). One can easily find that for close mode frequencies ($\Delta_s \simeq \Delta$) and their identical axial structures ($f_s(\zeta) = f(\zeta)$), $\xi_2 = 2\xi_{1,3} = 2\beta$ (cf. (38) and (42)).

The coefficients ξ_s , as well as the coefficients β_s and $\gamma_{ss'}$ (38), can be rather simply calculated analytically for a gyrotron with a constant amplitude of the RF field along the resonator axis $f_s(z) = \frac{1}{z_{out}}$ ($0 < z \leq z_{out}$). The corresponding dependences of the coefficients ξ_s and $\gamma_{ss'}$ on the transit angle are shown in Figs. 15 and 16. The transit angle of the central mode $\Theta_2 = \Delta_2 z_{out}$ is given in Fig. 15a-c along the horizontal axis; the mismatch δ is proportional to the distance between the mode frequencies: for the first mode (Fig. 15a), $\delta = \frac{\omega_2 - \omega_1}{\omega_2 - \omega_{H_0}}$, for the third mode, $\delta = \frac{\omega_3 - \omega_2}{\omega_2 - \omega_{H_0}} \approx \delta_{(1)}$. The designations in Fig. 16 correspond to the ones accepted in Fig. 11b.

In a simple case of three mode interaction, the phase-amplitude interaction of these modes can be described by the equations for the mode amplitudes and the phase difference $\bar{\Psi}$, that follow from (9), (10) and (41) [13]:

$$\begin{aligned} \frac{dF_1}{dt} &= F_1 (\sigma_1 - \beta_1' F_1^2 - \gamma_{12}' F_2^2 - \gamma_{13}' F_3^2) - F_3 \cdot F_2^2 \cdot \text{Re}(\xi_1 e^{-i\bar{\Psi}}), \\ \frac{dF_2}{dt} &= F_2 [\sigma_2 - \beta_2' F_2^2 - \gamma_{21}' F_1^2 - \gamma_{23}' F_3^2 - F_1 F_3 \cdot \text{Re}(\xi_2 e^{i\bar{\Psi}})], \\ \frac{dF_3}{dt} &= F_3 (\sigma_3 - \beta_3' F_3^2 - \gamma_{31}' F_1^2 - \gamma_{32}' F_2^2) - F_1 F_2 \cdot \text{Re}(\xi_3 e^{-i\bar{\Psi}}), \\ \frac{d\bar{\Psi}}{dt} &= \tilde{\delta} - F_1^2 (\beta_1'' + \gamma_{31}'' - 2\gamma_{21}'') - F_3^2 (\beta_3'' + \gamma_{13}'' - 2\gamma_{23}'') + F_2^2 (2\beta_2'' - \gamma_{12}'' - \gamma_{32}'') - \\ &\quad - \frac{F_3}{F_1} F_2^2 \cdot \text{Im}(\xi_1 e^{-i\bar{\Psi}}) - \frac{F_1}{F_3} F_2^2 \cdot \text{Im}(\xi_3 e^{-i\bar{\Psi}}) + 2F_1 F_3 \cdot \text{Im}(\xi_2 e^{i\bar{\Psi}}). \end{aligned} \quad (43)$$

We assumed here that the coupling impedances of all modes are equal, $\tilde{\delta} = \frac{\omega_1 + \omega_3 - 2\omega_2}{I_2 \omega_2} + \alpha_1'' + \alpha_3'' - 2\alpha_2''$.

For a gyrotron with close frequencies of the interacting modes and identical axial structures of their fields (when

$\gamma_{ss'} = \xi_2 = 2\xi_{1,3} = 2\beta$), the set of equations (43) defines the equilibrium states of the oscillator, which for equal Q-factors of all modes and a negligibly small nonequidistance of their frequency spectrum ($\tilde{\delta} \rightarrow 0$) are as follows^{from [13]} :

- single-mode oscillations with the intensity $F^2 = \frac{\sigma}{\beta'}$;
- oscillations of both lateral satellites in the absence of the central mode $F_1^2 = F_3^2 = \frac{\sigma}{3\beta'}$, $F_2 = 0$;
- symmetric synphase three-mode oscillations $\bar{\psi} = 0$, $F_2^2 = \frac{\sigma}{5\beta'}$,
 $F_1^2 = F_3^2 = \frac{2\sigma}{15\beta'}$;
- asymmetric antisynphase three-mode oscillations $\bar{\psi} = \pi$,
 $F_2^2 = \frac{\sigma}{5\beta'}$, $F_1^2 = \frac{\sigma}{10\beta'} (3 \pm \sqrt{5})$, $F_3^2 = \frac{\sigma}{10\beta'} (3 \mp \sqrt{5})$.

The analysis of the stability of these equilibrium states shows that all multimode oscillations are unstable and the characteristic equation of the fourth order for the stability of single-mode oscillations implied by (43) has three roots with a negative real part and one root with a zero real part. The latter is indicative of the fact that the oscillator with single-mode oscillations of the central mode does not react on the appearance of lateral satellites with small amplitudes $F_1 = F_3$ and the phase difference $\bar{\psi} = \pi$, i.e. on the auto-modulation with a frequency $\sim |\omega_2 - \omega_1|$ of the central mode oscillations. Therefore, the single-mode oscillations of the central mode can be considered here to be relatively stable (this conclusion is also supported by the results of numerical computations of eqs.(43)). However, we believe that such a stability can be changed as a result of weak variation in the gyrotron parameters.

The difference in the mode Q-factors can, no doubt, affect this stability. Let us suppose that the diffraction Q of the lateral satellites is smaller than that of the central mode

owing to electrodynamic selection and the beam current exceeds the starting value only for the central mode (i.e. $G_2 > 0$, $G_1 = G_3 < 0$). The satellite intensities in such an oscillator become equal as the time grows and the set of equations (43) with the given above relations for the coefficients γ_{ss} , $\gamma_{ss'}$, β_s and $F_1 = F_3$ taken into account, reduces to the form

$$\begin{aligned} \frac{dx}{d\tau} &= x \left[\gamma - \frac{r}{2} (x^2 + 3y^2 + 12z) \right] + y(z - 1 + x^2), \\ \frac{dy}{d\tau} &= y \left[\gamma - \frac{r}{2} (-x^2 + y^2 + 4z) \right] + x(3z + 1 - x^2), \end{aligned} \quad (44)$$

$$\frac{dz}{d\tau} = z \left[-\nu - x \cdot y - r \left(3z + \frac{3x^2 + y^2}{2} \right) \right]$$

Here $x = \sqrt{2F_2/|\delta|} \cos \frac{\Psi}{2}$, $y = \sqrt{2F_2/|\delta|} \sin \frac{\Psi}{2}$, $z = \frac{F_{1,3}^2}{|\delta|}$, $\tau = |\delta| I_0 \omega_0 t$, $\gamma = \frac{G_2}{|\delta|}$, $\nu = \left| \frac{G_{1,3}}{\delta} \right|$, $r = \beta' / \beta''$. The first two equations in set (44) define the stationary amplitude of the central mode (when $\frac{d}{d\tau} = 0$)

$$x^2 + y^2 = \frac{2\gamma}{r}, \quad x_{\pm}^2 = \frac{1}{1+r} \left[1 + \gamma r \pm \sqrt{(1 + \gamma r)^2 - 1 - r^2} \right].$$

The analysis of stability of these equilibrium states shows that only the equilibrium state with x_- is stable with respect to the variations in $\bar{\Psi}$ (or \tilde{x} and \tilde{y}). It follows from the last equation in set (44) that this equilibrium state is unstable with respect to the appearance of satellites when the condition

$$\nu < \frac{1}{r} \sqrt{2\gamma r + \gamma^2 r^2 - r^2} - 2\gamma$$

is fulfilled. This condition of automodulation instability shows that as the Q-factor of the satellites decreases (the parameter ν increases), the stability of the single oscillations of the central mode becomes better. This condition can

be also written in the form

$$\Upsilon < \frac{2\gamma}{1+\nu^2+4\nu\gamma+3\gamma^2}$$

which gives a better illustration of the difference between the example under study and the model analysed in [42], where the system with $\Upsilon = 0$ was considered. It was shown in [42] that automodulation oscillations, in which the growth of the central mode is stabilized by its decay into two passive satellites, can be stable besides the single oscillations of the central mode, depending on the relations between the increments of the central mode \mathcal{G}_2 and the decrements of the satellites $\mathcal{G}_{1,3}$. Moreover, it was shown that not only stable automodulation but also automodulation with a periodic change in the automodulation amplitude and stochastic oscillations can take place in such an oscillator. The active nonlinearity that is taken into account in eqs.(44) by the coefficient β'_s , as follows from the given condition of stability, makes the oscillator dynamics more regular because it becomes possible to stabilize the growth of the central mode by its own saturation.

Another factor that can influence the gyrotron dynamics is the difference in the mode frequencies, which causes the dispersion of the gyrotron nonlinear properties. Let us consider the interaction of three modes with equal Q-factors and the transit angles equal to $\Theta_1 = \pi$, $\Theta_2 = \frac{7}{6}\pi$, $\Theta_3 = \frac{4}{3}\pi$. In such an oscillator, as follows from Figs.11 and 12, the competition of two first modes takes place ($\gamma'_{12} \cdot \gamma'_{21} > \beta'_1 \cdot \beta'_2$); at the same time, the first mode that has the largest increment can maintain the third one that is in the hard self-excitation zone.

The results of the integration of the set of equations (43)

are presented in Fig.17 [13]. The values of the coefficients α_s , β_s , γ_{ss} and ξ_s are taken from Figs.11,15 and 16 for the given transit angles of the modes. As the beam current grows, the oscillator dynamics becomes more complicated (cf. Fig.17). When the beam current slightly exceeds the threshold value Fig.17a, $I/I_{st}^{min}=1.1$; $\tilde{\delta}=0$), stable oscillations of the first mode that has the lowest starting current are established. For a larger beam current ($I/I_{st}^{min}=1.2$, Fig.17b), the amplitude of the first mode becomes greater and, correspondingly, amplitude pulsations appear in the oscillations of the third, damping, mode (at the same time, the first mode suppresses the second one owing to the mode competition effect). Then, for $I/I_{st}^{min}=1.25$ (Fig.17c), the first mode provokes nonlinear excitation of the third mode and these two modes provoke pulsations of the second mode due to the phase coupling. At last, for $I/I_{st}^{min}=1.3$ (Fig.17d) and larger currents ($I/I_{st}^{min}=3$, Fig.17e), intense intermode beatings are established by the three-mode oscillations with constant amplitudes and phase $\bar{\Psi}$, i.e. mode locking takes place. A gyrotron with a slightly non-equidistant spectrum of eigenfrequencies behaves in a similar manner (see Fig.17f,g where $\tilde{\delta} \neq 0$).

Thus, due to the third mode whose role is here analogous to the role of a saturable absorber used for mode locking in lasers, the competition of two first (active) modes ceases to be dominant in the nonlinear interaction of modes.

Note, however, that in our study the mode locking remained stable even if the beam current exceeded the minimum threshold value by 5-10 times. These results disagree with the data by other authors [43,44] who carried out a space-time analysis of other microwave oscillators and showed that, when the beam

current is much larger than the minimum threshold value, mode locking is changed by stochastic oscillations. It is shown below that this disagreement can be explained by the fact that until recently we have not taken into account the change in the mode amplitude at times comparable with the transit time of electrons $T = L/v_{||}$. Such changes can be significant for large beam currents under the conditions of electron rebunching in a too strong RF field of the resonator and, hence, the delay effects that usually complicate the microwave oscillator dynamics [43,44] may become essential.

Space-Time Analysis of Nonstationary Processes in Multimode Gyrotrons

We have considered nonlinear effects in multimode gyrotrons using the mode representation of the resonator RF field. It is obvious, however, that this method is too complicated for the description of the processes in overmoded resonators with a large number of interacting modes. In such cases it seems reasonable to use space-time consideration of the resonator RF field describing this field as waves with slowly varying envelopes (without its representation as a sum of the resonator eigenmodes). A complex space-time structure of such an envelope seems to correspond to the excitation of a large number of eigenmodes.

Below, we shall describe briefly a series of problems which can be investigated using this space-time consideration.

A gyrotron with a whispering gallery wave

If the resonator radius is so large that the distance between the mode frequencies determined by relation (6) (see Lecture 1) is much smaller than the cyclotron amplification band (5),

many modes can be excited simultaneously. Let us represent the RF field of such a resonator in the form

$$\vec{E} = \text{Re} \left\{ \vec{e}(R_1) f(z) A(t, \varphi) e^{i(\omega t - m\varphi)} \right\},$$

where ω and φ define the basic frequency and the "basic" azimuthal index, respectively, and the function $A(t, \varphi)$ describes slow evolution of the wave envelope in both these variables:

$$\left| \frac{\partial A}{\partial t} \right| \ll \omega |A|, \quad \left| \frac{\partial A}{\partial \varphi} \right| \ll m |A| \quad (\text{see Fig.18}).$$

The self-consistent set of equations that describes such a system consists of the equation of electron motion (7) in the right-hand part of which $F(\varphi, t)$ should be written, the expression for the factor of excitation (11a) and the equation of the RF field excitation which follows from the Maxwell equations and can be written in the form [44]

$$\frac{\partial F}{\partial \tau} + \frac{\partial F}{\partial \varphi} + F = F \cdot \Phi.$$

This equation must be supplemented with the initial condition $F(\tau=0) = F_0(\varphi)$ and the condition of the RF field periodicity along the cyclic coordinate $F(\varphi) = F(\varphi + 2\pi)$.

Preliminary results of the numerical investigation of such a set of equations showed that, if the beam current does not exceed the threshold value too much, the oscillations with a constant amplitude along φ are established (this fact corresponds to one mode excitation). Then, for a larger beam current, the azimuthal structure of the envelope becomes nonhomogeneous but the envelope remains stable in time, which corresponds to the mode locking analysed above.

A quasioptical gyrotron

It was mentioned in the first lecture that in recent years the possibility of using two-mirror quasioptical resonators (similar to the ones used in lasers) in gyrotrons have been actively analysed. The theory of stationary oscillations in

such quasioptical gyrotrons was developed in [6,46]. The numerical study of nonstationary processes in such systems with a large number of excited modes was provided in [7]. We shall consider here the results of investigations of similar processes that were obtained using the space-time approach [47].

Let us represent the RF field of the resonator shown in Fig.19 as a sum of two waves moving between the mirrors in the opposite directions

$$\vec{E} = \text{Re} \left\{ E(x, z) \vec{x}_0 e^{i\omega t} \left[A_+(t, \gamma) e^{-iky} + A_-(t, \gamma) e^{iky} \right] \right\}.$$

We assume that all losses of the microwave power in the resonator are caused by the fact that the coefficient of reflection of the direct wave at the output mirror is different from unity ($R < 1$). Taking into account the above-mentioned conditions of the slow change of the wave envelopes in t and along γ , one can easily reduce the Maxwell equations to the equations of excitation of the opposite waves

$$\frac{\partial F_+}{\partial \tau} + \frac{\partial F_+}{\partial \gamma} = \hat{\Phi}_+', \quad \frac{\partial F_-}{\partial \tau} - \frac{\partial F_-}{\partial \gamma} = \hat{\Phi}_-'$$

These equations should be supplemented with the boundary conditions $F_+(Y=0) = F_-(Y=0)$, $F_-(Y=L) = R F_+(Y=L)$ and the initial conditions $F_{\pm}(\tau=0) = F_{\pm}^{(0)}(\gamma)$. Now we put the sum of these two waves $F_+ e^{iy_+} + F_- e^{iy_-}$ into the right-hand part of the equation of electron motion (7) and replace the integration over the resonator cross-section in the expression for the factor of excitation $\hat{\Phi}_s$ (11a) by the averaging over the difference between the phases of the two opposite waves which varies by 2π at the wavelength in the γ -direction [47]. Thus the equations obtained will be the equations averaged over a small scale of the order of the wavelength in the γ -direction. Nevertheless, using these equations one can analyse the

slow evolution of the wave envelopes in time and along the Υ -coordinate.

The results of numerical investigations of such a system are presented in Fig.20. This figure shows the dependence of the wave amplitudes at the left mirror ($\Upsilon = 0$) on the "slow" dimensionless time $\tau = I_s \omega t$ for different values of the "beam current" variable $L' = I_s L$ (for the parameters corresponding to Fig.20, the threshold value of the parameter L' is $L' = 0.042$). It is seen from Fig.20a that, if the beam current slightly exceeds the starting value, stationary oscillations with a constant amplitude are established in this oscillator (the dashed lines in Fig.20 denote the electron orbital efficiency averaged over the interaction space $\bar{\eta}_\perp = \frac{1}{L'} \int_0^{L'} \eta_\perp d\Upsilon$). As the beam current grows, automodulation appears in these oscillations (Fig.20b) and the amplitude of the modulation increases with the current. Then, with a further increase in current, the oscillations with a periodically varying depth of automodulation appear and the modulation period doubles (Fig.20c). Finally, for still larger currents, the oscillations become stochastic (Fig.20d). The oscillator behaves in a similar manner for other values of the reflection coefficient: the results for $R = 0.8$ and $R = 0.9$ are given in Fig.20c, in all other figures, $R = 0.8$.

The space structure of the amplitudes of both waves in various regimes of operation is given in Fig.21a-d, where the discrete time points ($21 \leq \tau \leq 25$) that correspond to these pictures are marked and the values of the orbital efficiency $\bar{\eta}_\perp$ are given. As follows from these figures, a complex structure of the RF field is typical of stochastic oscillations in contrast to automodulation and regular oscillations (cf. Fig.

21a, b and d). A similar space structure with several maxima is also formed in stochastic oscillations in BWO [44].

A gyrotron with a nonfixed axial structure of the RF field

In order to enhance the output microwave power of a powerful gyrotron and to diminish the ohmic losses of microwave power in the resonator walls, it seems expedient to decrease the diffraction Q of the resonator. However, as the coefficient of the wave reflection at the output cross-section approaches zero and, correspondingly, the diffraction Q comes close to its minimum value that is determined by the resonator length $Q_{dif}^{min} \approx 8\pi(L/\lambda)^2$, the axial structure of the RF field in such a resonator becomes nonfixed and is established in a self-consistent manner upon the influence of the electron beam.

The theory of stationary oscillations in a gyrotron with a nonfixed axial structure of the resonator field was developed in [48], where it was shown, in particular, that the orbital efficiency of oscillations in such gyrotrons can be as high as $\eta_{\perp}^{max} = 75\%$. Below, we shall describe in brief the equations of a similar nonstationary theory and preliminary results of its investigation [49].

Taking into account the fact that the frequency of oscillations is close to the cut-off frequency ω_0 of a part of the waveguide that is used as a resonator, one can represent a nonstationary RF field in the form

$$\vec{E} = \text{Re} \{ A(z, t) \vec{E}_s(\vec{R}_\perp) e^{i\omega_0 t} \},$$

where the function $\vec{E}_s(\vec{R}_\perp)$ describes a fixed transverse structure of the electric field, $A(z, t)$ is the complex amplitude of the RF field that varies slowly in time and along the axial coordinate \bar{z} .

Substituting this representation into the Maxwell equations and taking the condition of slow variation of the amplitude in time $|\frac{\partial A}{\partial t}| \ll \omega |A|$ into account, one can easily obtain a parabolic equation that describes the excitation of the RF field by the electron beam. In terms of variables of the gyrotron theory this equation has the form

$$\frac{\partial^2 f}{\partial \xi^2} - i \frac{\partial f}{\partial \tau} = \frac{I_0}{2\pi} \int_0^{2\pi} a^* d\vartheta_0. \quad (45)$$

Here $\tau = \frac{\beta_{\perp 0}^4}{8\beta_{\parallel 0}^2} \omega_0 t$ is a "slow" time, the beam current parameter I_0 corresponds to the expression given in [47]:

$$I_0 = 16 \frac{e|I|}{m_0 c^3} \cdot \frac{\beta_{\parallel}}{\beta_{\perp}^6} J_{m \pm n}^2(kR_0) [(\nu^2 - m^2) J_m^2(\nu)]^{-1}.$$

The boundary conditions for the resonator that is formed by a part of a regular waveguide with a cut-off narrowing in the input cross-section and whose output cross-section is determined by the ceasing of the interaction between the electrons and the RF field due to a sharp change in the external magnetic field, can be given in the form

$$f|_{\xi=0} = 0, \quad \frac{\partial f_{\omega}}{\partial \xi} \Big|_{\xi=\xi_{out}} = -i k_{\parallel} f_{\omega}.$$

Here the second condition is the condition of radiation of the Fourier components f_{ω} of the resonator nonstationary field $f = \int_0^{\infty} f_{\omega} \exp\{i[(\omega - \omega_0)t - k_{\parallel}z]\} d\omega$, $k_{\parallel} = \frac{1}{c} \sqrt{\omega^2 - \omega_0^2}$ is the axial wavenumber.

Preliminary results on the study of the self-consistent set of equations (7) and (45) are presented in Fig.22. The calculations were carried out for $\xi_{out} = 10$, the negative frequency mismatch $\Delta = -0.6$ corresponds to the synchronism between the electrons and the components of the RF field that propagate in the direction opposite to the direction of the

electron axial velocity; the latter fact enhances the feedback in such an oscillator. It is shown in Fig.22 that with an increase in the beam current the time of the transitional non-stationary period grows; after this period oscillations with a constant amplitude are established. Figure 22b shows that auto-modulation oscillations are established at a large beam current. A rather low efficiency of oscillations can be explained by the fact that the axial structure of the resonator field is unfavourable for efficiency, which is typical of the resonance with opposite waves when the amplitude of the RF field is maximum near the input cross-section. An example of the axial structure of the RF field under such a gyrotron operation is given in Fig.23.

Conclusion

Our consideration testifies to the fact that the effects of mode interaction in gyrotrons have received a thorough study so that we have understood the physical reasons for the appearance of these effects in gyrotrons. We believe that the developed theory can be applied to the computation of the processes in gyrotrons where several modes can be self-excited.

At the same time, the investigation of nonstationary processes in gyrotrons with overmoded resonators where a lot of modes can be excited is in its early stage. The basic mechanisms that cause the complication of oscillations in such gyrotrons can be considered known in view of the results obtained in the analysis of nonstationary processes in gyrotrons and other microwave devices (free electron lasers, backward wave oscillators and others). Nevertheless, this range of problems seems to be an attractive field for fruitful theoretical investigations.

REFERENCES

1. Vlasov, S.N. et al. Radiophysics and Quantum Electronics, 1969, 12, 8, 972.
2. Vlasov, S.N., Zagryadskaya, L.N., and Orlova, I.M. Radiotekhnika i Elektronika, 1976, 21, 7, 1485.
3. Antakov, I.I. et al. Elektronnaya Tekhnika, Ser.1, Elektronika SVCh, 1975, N8,20.
4. Luchinin, A.G. and Nusinovich, G.S. Elektronnaya Tekhnika, Ser.1, Elektronika SVCh, 1975, N11, 26.
5. Vainstein, L.A. Open Resonators and Open Waveguides, translated by P.Beckmann, Boulder: Golem Press, 1969.
6. Sprangle, P., Vomvoridis, J.L., and Manheimer, W.M. Phys. Rev. A, 1981, 23, 3127.
7. Bondeson, A. et al. Int. J. Electronics, 1982, 53, 6, 547.
8. Carmel, Y et al. Phys. Rev. Lett., 1983, 50, 2, 112.
9. Zapevalov, V.E. et al. X All-Union Conf. on Microwave Electronics, Conf. Digest, Minsk, USSR, 1983, p.12.
10. Gaponov, A.V., Petelin, M.I., and Yulpatov, V.K. Radiophysics and Quantum Electronics, 1967, 10, 9-10, 794.
11. Flyagin, V.A. et al. IEEE-MTT, 1977, MTT-25, 6, 514.
12. Moiseev, M.A. and Nusinovich, G.S. Radiophysics and Quantum Electronics, 1974, 17, 11, 1305.
13. Nusinovich, G.S. Int. J. Electronics, 1981, 51, 4, 457.
14. Van-der-Pol, B. Phyl. Mag., 1922, 43, 700.
15. Andronov, A.A. and Vitt, A.A. ZhTP, 1934, 4, 1, 122.
16. Skibarko, A.P. and Strelkov, S.P. 1934, 4, 1, 158.
17. Lamb, W.E. Phys. Rev. A, 1964, 134, 6a, 1429.
18. Vainstein, L.A. In: High Power Electronics, ed. by Nauka, Moscow, 1969, v.6, 84.

19. Vainstein, L.A. and Solntsev, B.A. Lectures on Microwave Electronics, ed. by Soviet Radio, Moscow, 1972.
20. Nusinovich, G.S. In: Gyrotron, ed. by the Institute of Appl. Phys. Acad. Sci. of the USSR, Gorky, 1981, 146.
21. Kurayev, A.A. Microwave Devices with Periodical Electron Beams, Minsk, USSR, 1971.
22. Moiseev, M.A. and Nusinovich, G.S. In: Gyrotron, ed. by the Institute of Appl. Phys. Acad. Sci. of the USSR, Gorky, 1981, 41.
23. Zarnitsyna, I.G. and Nusinovich, G.S. Radiophysics and Quantum Electronics, 1974, 17, 12, 1418.
24. Nusinovich, G.S. and Zapevalov, V.E. Radiotekhnika i Elektronika, 1984, 29, 11.
25. Flyagin, V.A. and Nusinovich, G.S. Report at the 8th Int. Conf. on Infrared and Millimeter Waves, Miami Beach, Florida, USA, Dec. 1983, Infrared and Millimeter Waves, ed. by Academic Press, v.13, 1985.
26. Nusinovich, G.S. Elektronnaya Tekhnika, Ser.1, Elektronika SVCh, 1974, 3, 44.
27. Kreisler, K.E. and Temkin, R.J. Int. J. Infrared and Millimeter Waves, 1981, 2, 2, 175.
28. Petelin, M.I. and Yulpatov, V.K. Radiophysics and Quantum Electronics, 1975, 18, 2, 212.
29. Petelin, M.I. In: Gyrotron, ed. by the Institute of Appl. Phys. Acad. Sci. of the USSR, Gorky, 1981, 5.
30. Jory, H.R. Report at the 4th Int. Symp. on Heating in Toroidal Plasmas, Rome, Italy, March 1984.
31. Zapevalov, V.E., Korablev, G.S., and Tsimring, Sh.E. Radiotekhnika i Elektronika, 1977, 22, 8, 1661.
32. Gol'denberg, A.L. and Petelin, M.I. Radiophysics and Quantum Electronics, 1973, 16, 1, 106.
33. Tsimring, Sh.E. Radiophysics and Quantum Electronics, 1972, 15, 8, 952.

34. Nusinovich, G.S. and Erm, R.E. Elektronnaya Tekhnika, Ser.1, Elektronika SVCh, 1972, 8, 55.
35. Flyagin, V.A., Gol'denberg, A.L., and Nusinovich, G.S. Infrared and Millimeter Waves, ed. by Academic Press, v.11, 1984.
36. Zarnitsyna, I.G. and Nusinovich, G.S. Radiophysics and Quantum Electronics, 1975, 18, 2, 223.
37. Nusinovich, G.S. Radiophysics and Quantum Electronics, 1976, 19, 12, 1301.
38. Smith, J.M. Models in Ecology, Cambridge University Press, 1974.
39. Zapevalov, V.E. and Nusinovich, G.S. Izv. VUZov, Radiofizika, 1984, 27, 1, 117;
Nusinovich, G.S. In: Infrared and Millimeter Waves, ed. by Academic Press, 1984, v.11.
40. Kreischer, K.E. et al. Plasma Fusion Center, MIT, USA, PFC/JA-82-34, Dec. 1982.
41. Zarnitsyna, I.G. and Nusinovich, G.S. Radiophysics and Quantum Electronics, 1977, 20, 3, 313.
42. Rabinovich, M.I. and Fabrikant, A.L. ZhETP, 1979, 77, 2, 617.
43. Bogomolov, Ya.L. et al. Optics Commun., 1979, 32, 3, 209.
44. Ginzburg, N.S., Kuznetsov, S.P., and Fedoseeva, T.N. Izv. VUZov, Radiofizika, 1978, 21, 7, 1037.
45. Petelin, M.I. In: Gyrotron, ed. by the Institute of Appl. Phys. Acad. Sci. of the USSR, Gorky, 1981, 77.
46. Zarnitsyna, I.G. and Nusinovich, G.S. Radiotekhnika i Elektronika, 1978, 23, 6, 1212.
47. Nusinovich, G.S. and Sher, E.M. Int. J. Electronics, 1984, 56, 3, 275.
48. Bratman, V.L., Moiseev, M.A., Petelin, M.I., and Erm, R.E. Radiophysics and Quantum Electronics, 1973, 16, 4, 474.
49. Ginzburg, N.S., Zavolsky, N.A., Nusinovich, G.S., and Sergeev, A.A. Radiophysics and Quantum Electronics (to be published in 1985, 28).

FIGURE CAPTIONS

Fig. 1. Real part of ϕ_2 as a function of mismatch Δ_2 in a nonexcited oscillator (ϕ'_{2L}) and in the presence of the first mode ($F_1=0.04$), for various values of Δ_1 . The horizontal dashed lines show corresponding values of ϕ'_1 . (In the text the indices 1,2 are replaced by 0,1, respectively).

Fig. 2. (a) Single mode orbital efficiency versus beam current parameter I_0 , with Gaussian axial field structure and $\zeta_{out}=17$. for various values of Δ_1 .

(b) Amplitude of single mode oscillations F_1 as a function of mismatch Δ_1 for fixed $I_0=10^3$.

Fig. 3. Zone of parasitic self excitation in a gyrotron with constant beam current parameter $I_0=10^3$ and $q=1$, $\zeta_{out}=17$.

Fig. 4. Threshold values q_{th}^{-1} for parasitic mode at optimum values of the parameters for the operating mode.

Fig. 5. Beam current parameter vs mismatch for automodulation instability. solid curve: starting current for operating mode. dashed curve: optimum for electronic efficiency of operating mode. dash-dot curve: break in operating mode oscillations at edge of zone of hard self excitation. shaded curves: boundaries of zone of operating mode stability for different values of $\tilde{\Delta}$.

Fig. 6. Dependence of critical beam current for automodulation on distance $\tilde{\Delta}$ between mode frequencies. The mismatch Δ for the operating mode is fixed at the optimum value (0.6). solid shaded lines $q=1$. dashed lines $q=1/2$.

Fig. 7. Starting current vs. magnetic field for the $TE_{15,1,1}$ mode and neighboring competing modes. An idealized closed cavity of length 4λ ($=1.2$ cm at 100 GHz) is employed. All modes have a loaded Q of 100 (from [30]).

Fig. 8. self excitation zones (solid curve) and voltage trajectories (dashed curves) of modes resonant with the fundamental cyclotron harmonic for parameters $I_0, \zeta_{out}, \Delta_{op}=0.4$ corresponding to the maximum electronic efficiency in the plane $x=\frac{1}{2}\beta_1^2, y=\frac{1}{2}\beta^2$. The shaded region corresponds to self excitation of the operating mode. Trajectory I: equal voltages at anode and resonator. Trajectory II: constant voltage difference between anode and resonator. (a): competing modes well separated from operating mode; (b) denser frequency spectrum of competing modes.

Fig. 9. Starting current vs resonator voltage with equal voltage pulses at anode and resonator for the $TE_{15,1,1}$ mode.

Fig. 10. Phase portrait of oscillator. (a) strong coupling between modes. (b) weak coupling between modes.

Fig. 11. (a) Real parts of the coefficients α, β versus transit angle $\theta=\Delta\zeta_{out}$ for a uniform field profile.

(b) Real parts of the coefficients χ_{ss} , versus θ_s for different values of the ratio $K=\theta_{s'}/\theta_s$.

Fig. 12. Lines of constant values of $\Psi=\chi'_{12}\chi'_{21}/\beta'_1\beta'_2$ in the plane of transit angles $\theta_s=\Delta\zeta_{out}, s=1,2$.

Fig. 13. Nonstationary processes in a gyrotron for three different values of the beam current, showing support of parasitic mode at very large currents.

Fig. 14. Field of parasitic self excitation in the plane of mismatches $\Delta_1, \tilde{\Delta}$ in a nonexcited oscillator (dashed lines) and in a gyrotron with oscillation amplitude $F_1 \neq 0$ (shaded).

Fig. 15. Real (solid) and imaginary (dashed) parts of the coefficients ξ_s for a three mode gyrotron as a function of transit angle θ_2 for three values of $\delta = (\omega_2 - \omega_1) / (\omega_2 - \omega_{H_0})$ (mode 2 is the central mode) and constant field profile.
(a) $s=1$; (b) $s=2$; (c) $s=3$

Fig. 16. Dependence of the coefficients γ_{ss} , and β_s on transit angle θ_2 for different values of the ratio $K = \theta_{s1} / \theta_s$.

Fig. 17. Amplitude and phase time evolution in a three mode gyrotron with relation between modes. a) $I/I_{st}^{\min} = 1.1, \delta=0$;
b) $I/I_{st}^{\min} = 1.2, \delta=0$; c) $I/I_{st}^{\min} = 1.25, \delta=0$;
d) $I/I_{st}^{\min} = 1.3, \delta=0$; e) $I/I_{st}^{\min} = 3.0, \delta=0$;
f) $I/I_{st}^{\min} = 3.0, \delta=1$; g) $I/I_{st}^{\min} = 3.0, \delta=2$.

Fig. 18. Cross section of a CRM showing rotating wave envelope A defined in lecture 4.

Fig. 19. Cross section of a CRM with counter-rotating waves in plane geometry.

Fig. 20. Time dependence of the wave amplitude at the left mirror for various values of the beam current variable.

Fig. 21. Spatial structure of both opposite waves at fixed moments in time $\tau = I\omega t$ for various values of the beam current variable.

Fig. 22. Time dependence of efficiency for various values of beam current parameter with $\delta = -0.6$ and $\zeta_{out} = 10$.

(a) $I=0.01, 0.02$ and 0.04 , showing the increase in duration of the nonstationary phase with increasing beam current.
(b) $I=0.1$, showing the onset of automodulation oscillations.

Fig. 23. Axial structure of resonator field at large values of the beam current parameter.

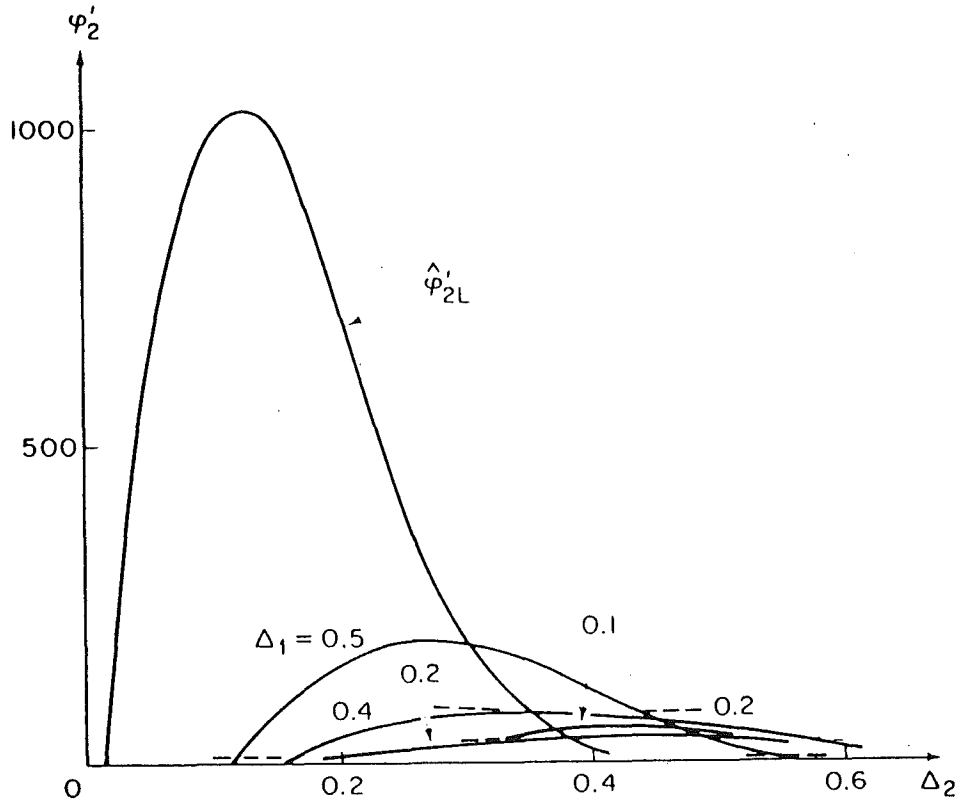


Fig. 1. Real part of $\hat{\phi}'_2$ as a function of mismatch Δ_2 in a nonexcited oscillator ($\hat{\phi}'_{2L}$) and in the presence of the first mode ($F_1=0.04$), for various values of Δ_1 . The horizontal dashed lines show corresponding values of $\hat{\phi}'_1$. (In the text the indices 1,2 are replaced by 0,1, respectively).

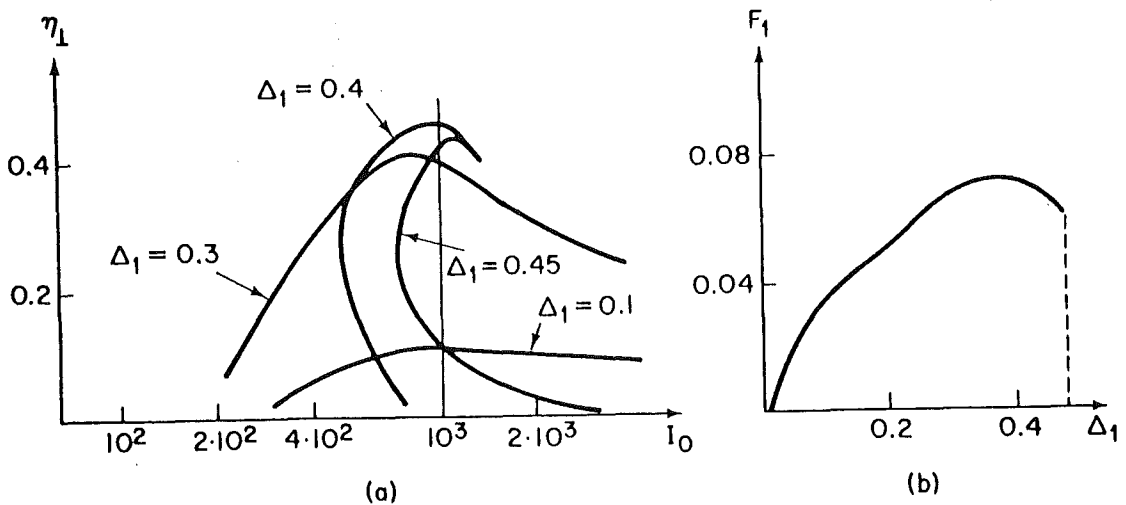


Fig. 2. (a) Single mode orbital efficiency versus beam current parameter I_0 , with Gaussian axial field structure and $\zeta_{out}=17$. for various values of Δ_1 .

(b) Amplitude of single mode oscillations F_1 as a function of mismatch Δ_1 for fixed $I_0=10^3$.

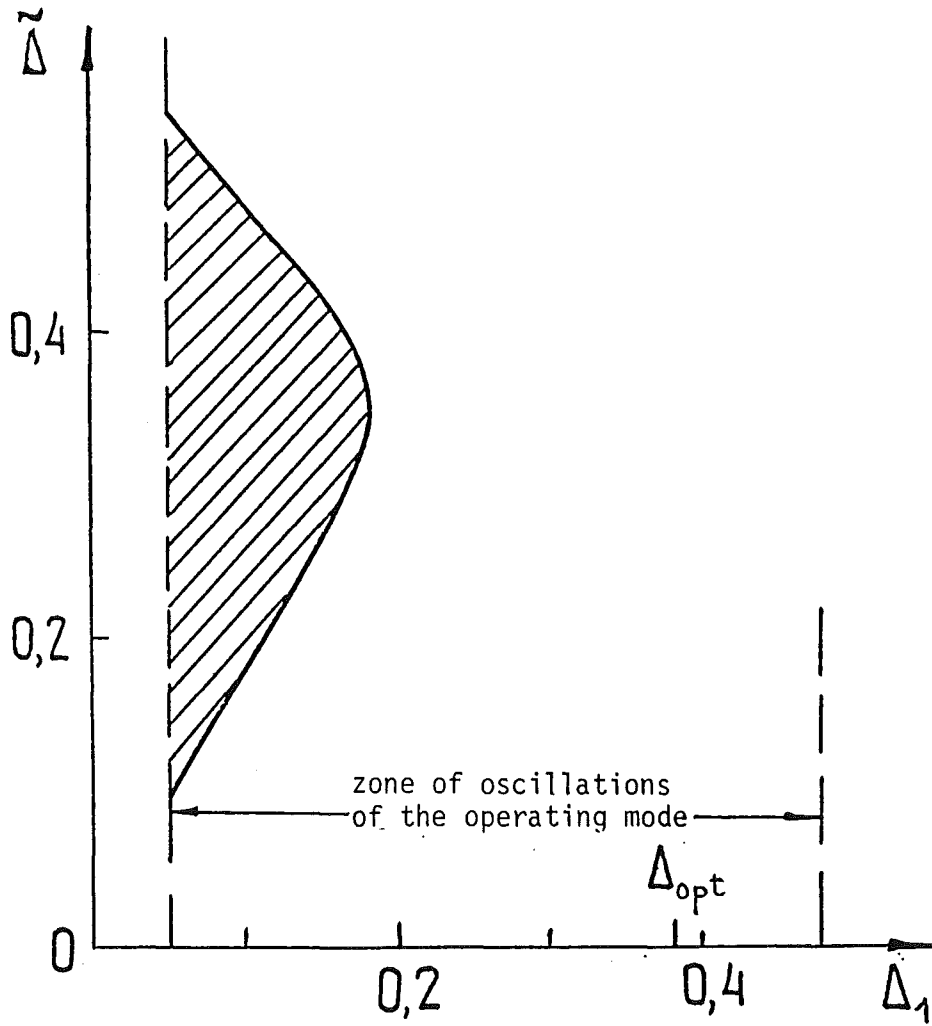


Fig. 3. Zone of parasitic self excitation in a gyrotron with constant beam current parameter $I_0=10^3$ and $q=1$, $\zeta_{out}=17$.

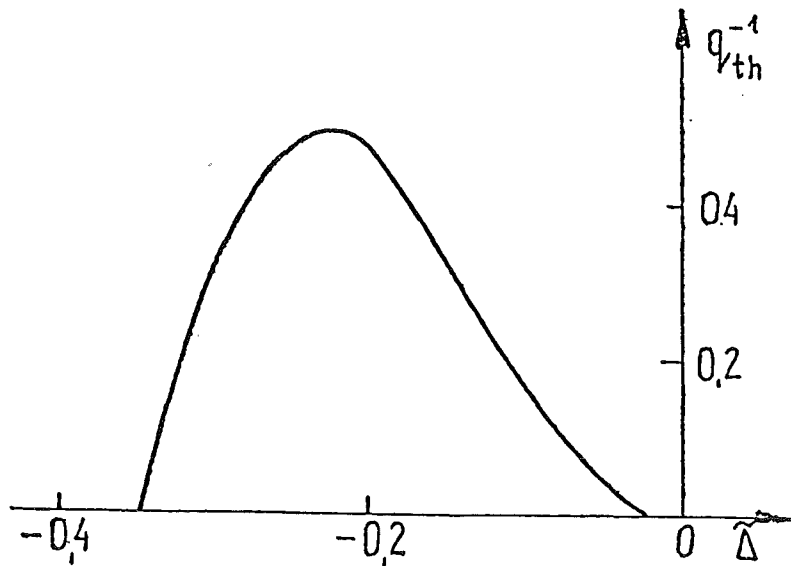


Fig. 4. Threshold values q_{th}^{-1} for parasitic mode at optimum values of the parameters for the operating mode.

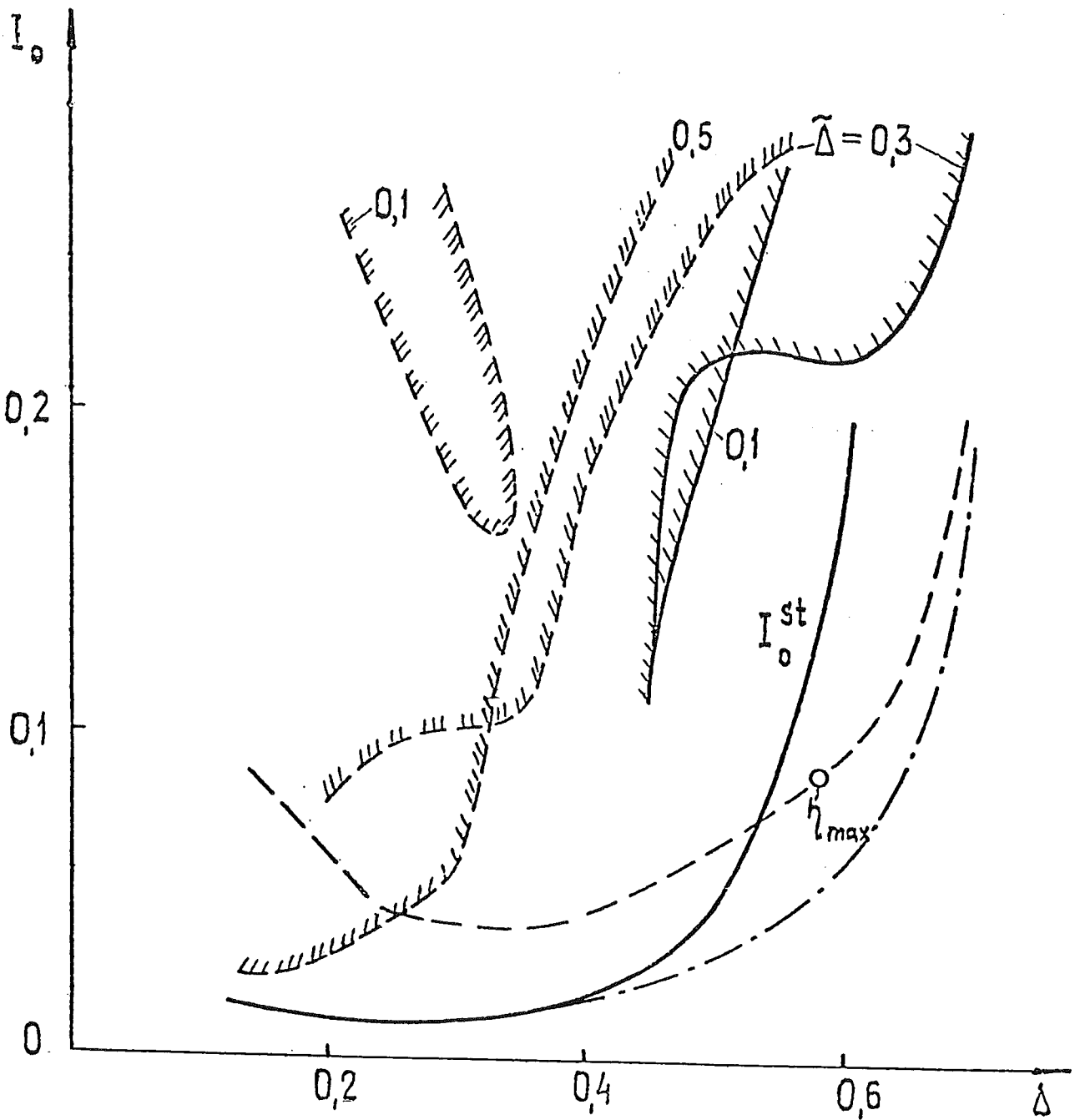


Fig. 5. Beam current parameter vs mismatch for automodulation instability. solid curve: starting current for operating mode. dashed curve: optimum for electronic efficiency of operating mode. dash-dot curve: break in operating mode oscillations at edge of zone of hard self excitation. shaded curves: boundaries of zone of operating mode stability for different values of $\tilde{\Delta}$.

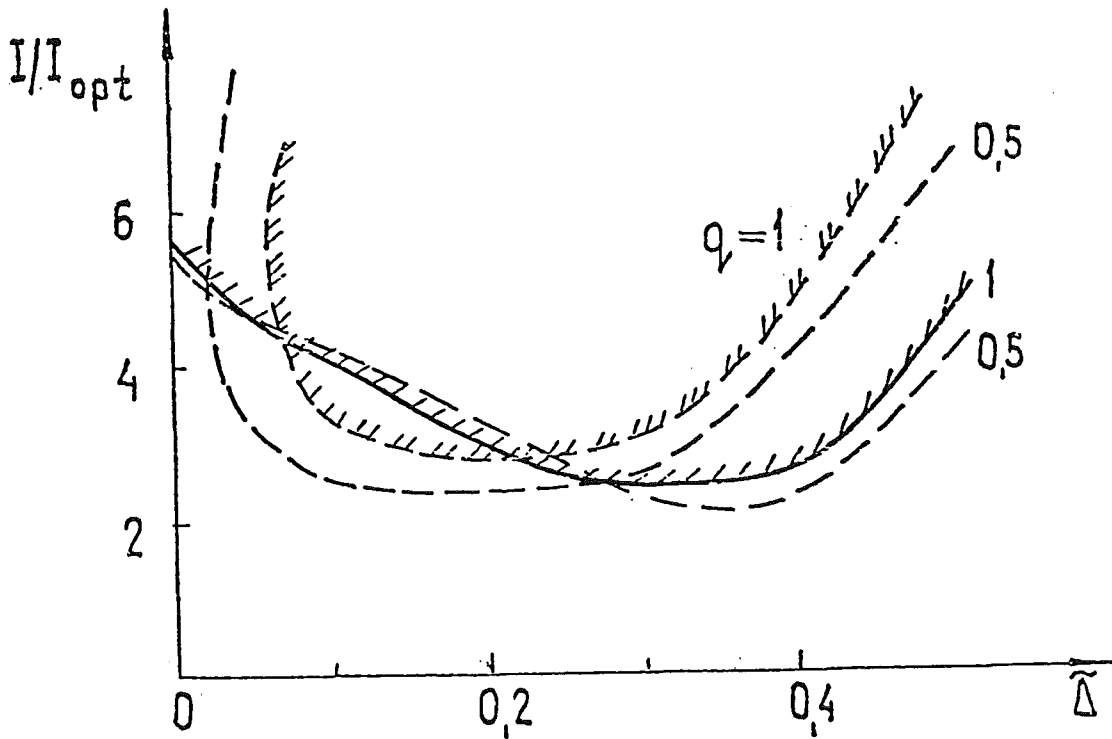


Fig. 6. Dependence of critical beam current for automodulation on distance $\tilde{\Delta}$ between mode frequencies. The mismatch Δ for the operating mode is fixed at the optimum value (0.6). solid shaded lines $q=1$. dashed lines $q=1/2$.

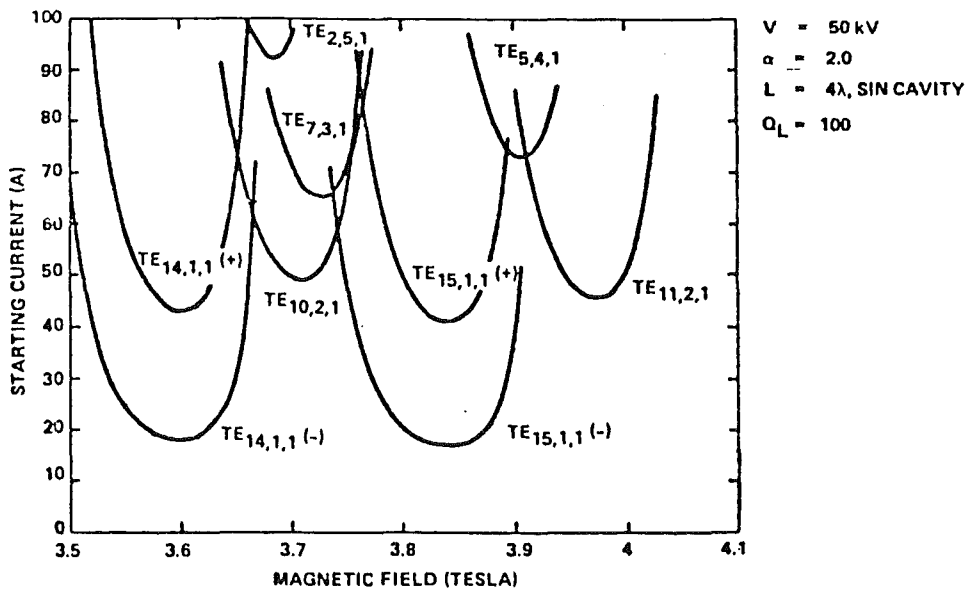


Fig. 7. Starting current vs. magnetic field for the $TE_{15,1,1}$ mode and neighboring competing modes. An idealized closed cavity of length 4λ ($=1.2$ cm at 100 GHz) is employed. All modes have a loaded Q of 100 (from [30]).

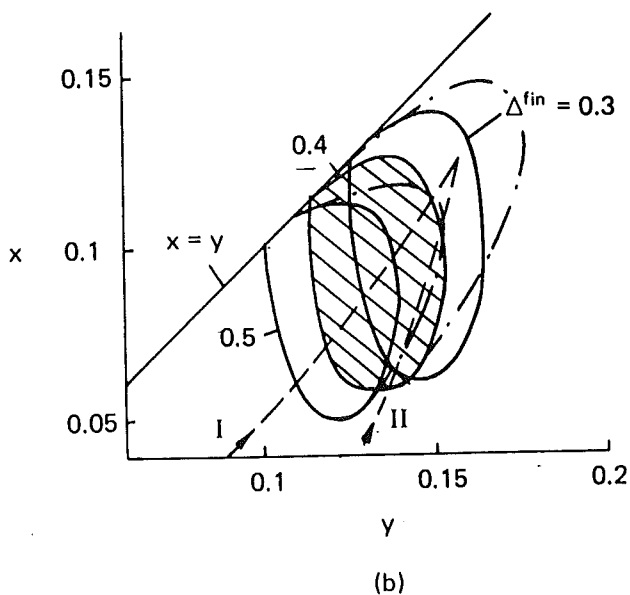
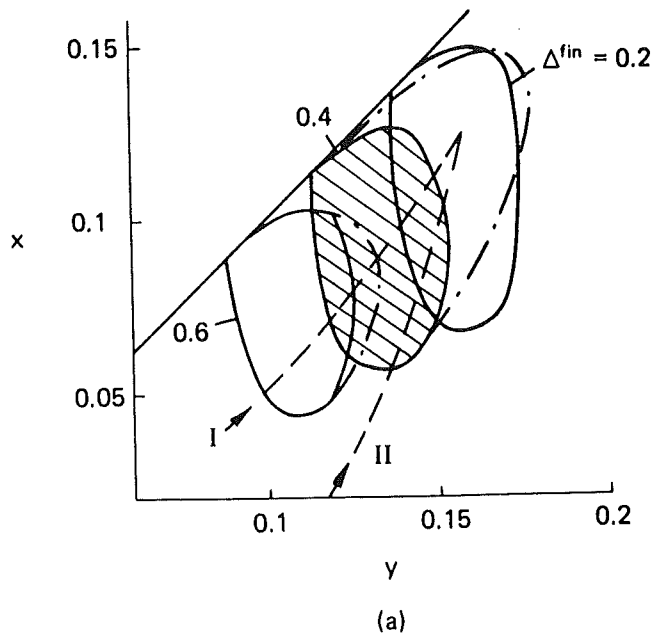


Fig. 8. self excitation zones (solid curve) and voltage trajectories (dashed curves) of modes resonant with the fundamental cyclotron harmonic for parameters $I_0, \zeta_{out}, \Delta_{op}=0.4$ corresponding to the maximum electronic efficiency in the plane $x=\frac{1}{2}\beta_{\perp}^2, y=\frac{1}{2}\beta^2$. The shaded region corresponds to self excitation of the operating mode. Trajectory I: equal voltages at anode and resonator. Trajectory II: constant voltage difference between anode and resonator. (a): competing modes well separated from operating mode; (b) denser frequency spectrum of competing modes.

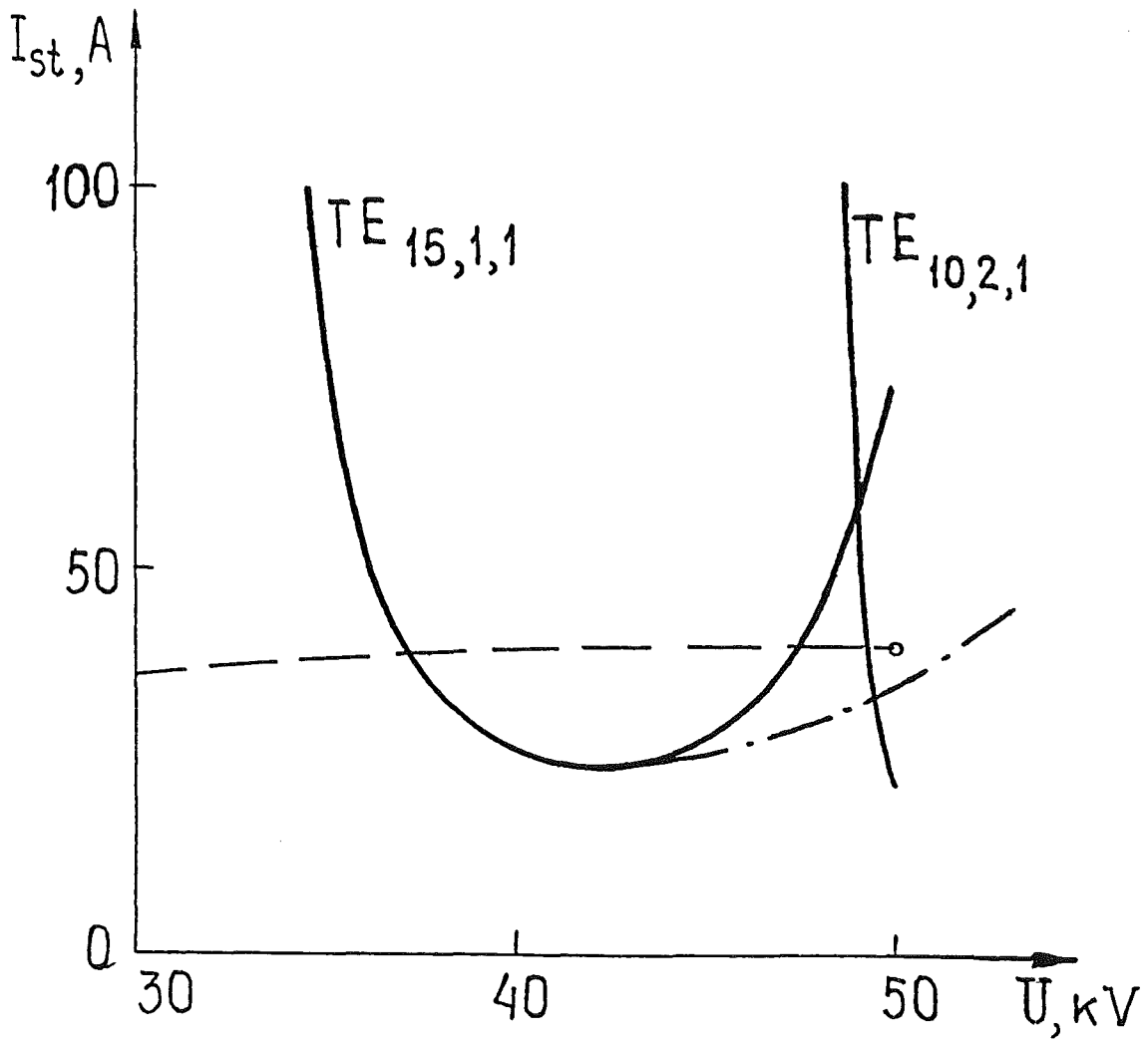


Fig. 9. Starting current vs resonator voltage with equal voltage pulses at anode and resonator for the $TE_{15,1,1}$ mode.

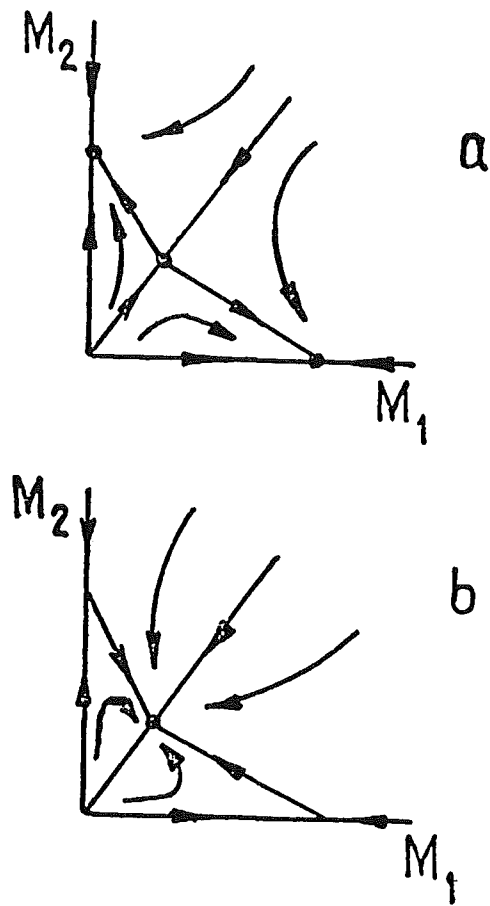


Fig. 10. Phase portrait of oscillator. (a) strong coupling between modes. (b) weak coupling between modes.

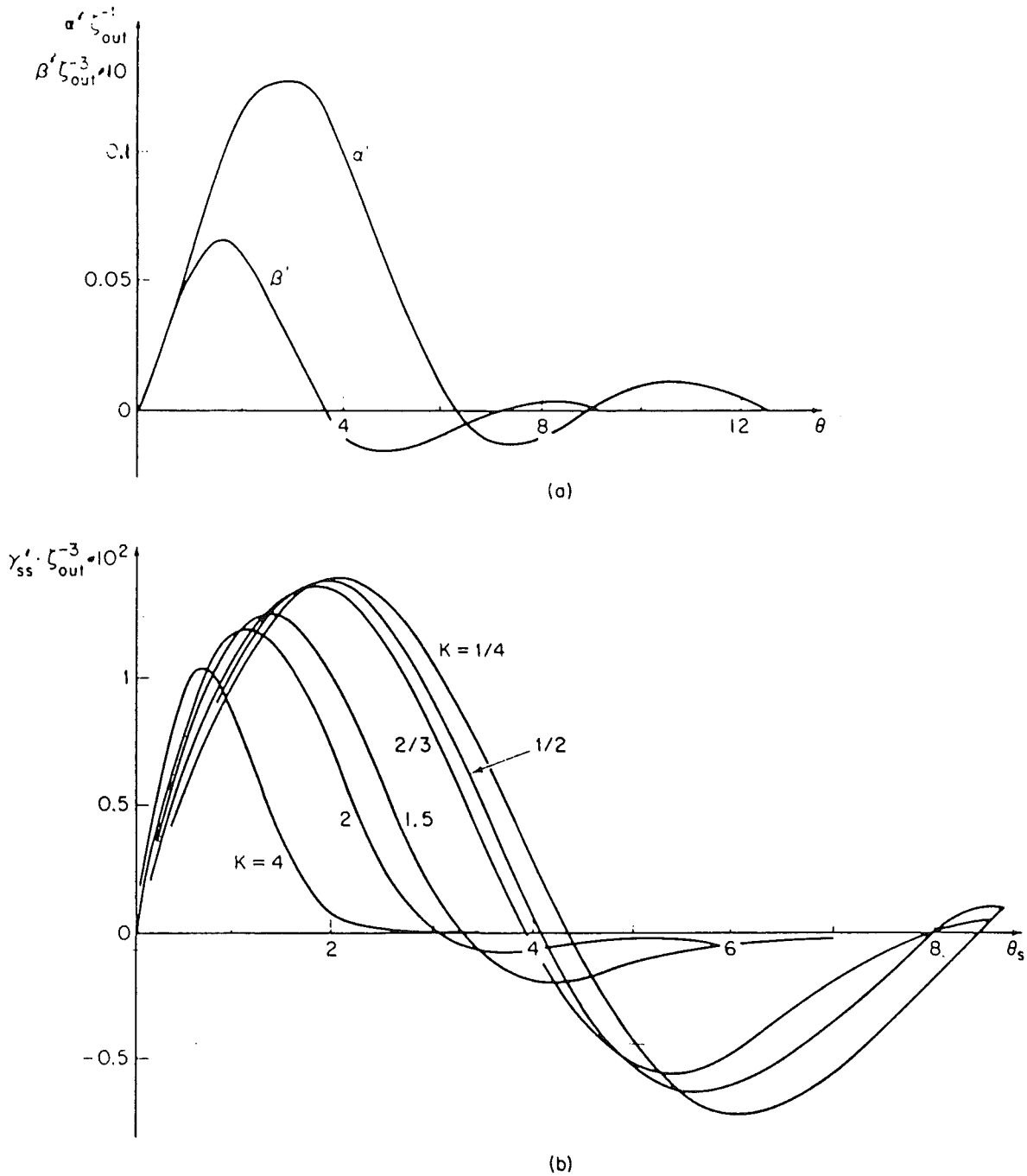


Fig. 11. (a) Real parts of the coefficients α, β versus transit angle $\theta = \Delta \zeta_{out}$ for a uniform field profile.

(b) Real parts of the coefficients γ_{ss}' , versus θ_s for different values of the ratio $K = \theta_{s1}/\theta_s$.

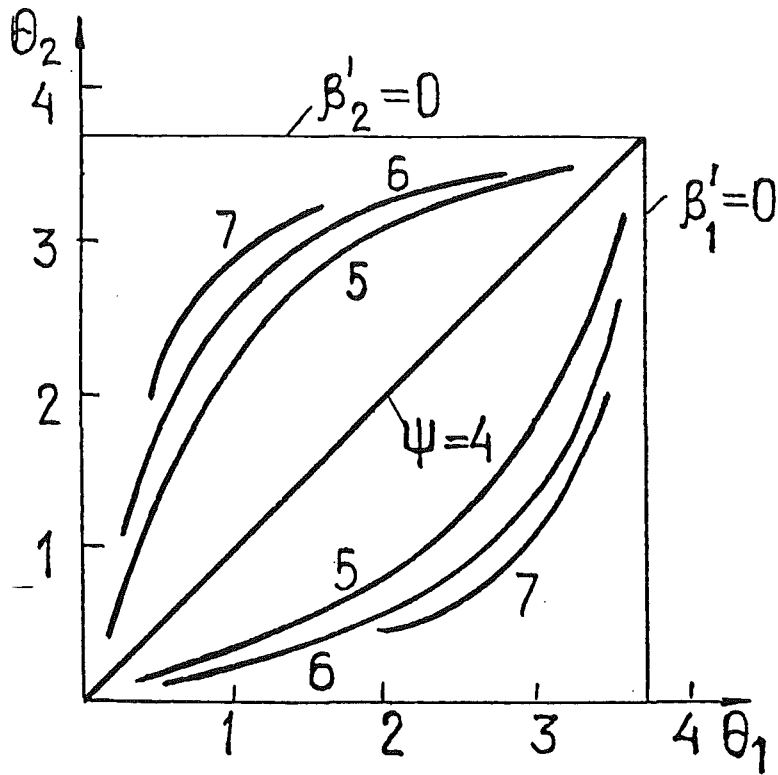


Fig. 12. Lines of constant values of $\Psi = \alpha'_{12} \alpha'_{21} / \beta'_1 \beta'_2$ in the plane of transit angles $\theta_s = \Delta_s \zeta_{out}$, $s=1,2$.

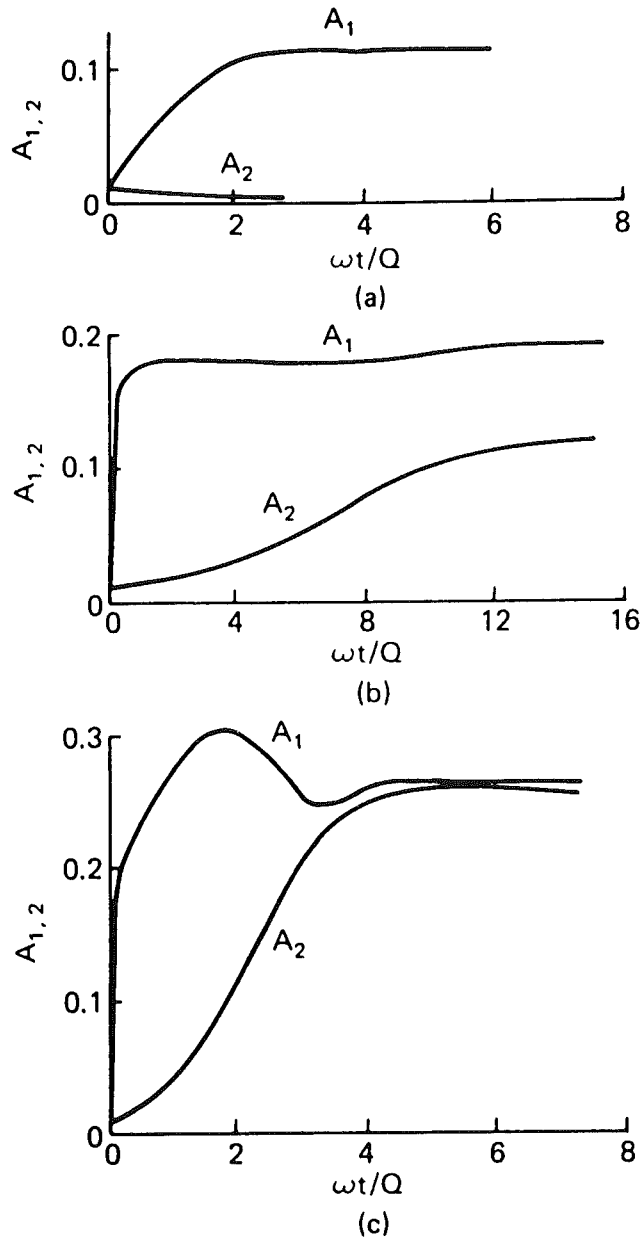


Fig. 13. Nonstationary processes in a gyrotron for three different values of the beam current, showing support of parasitic mode at very large currents. (a) $I/I_{st}^{(1)} = 7$; (b) $I/I_{st}^{(1)} = 32$; (c) $I/I_{st}^{(1)} = 110$.

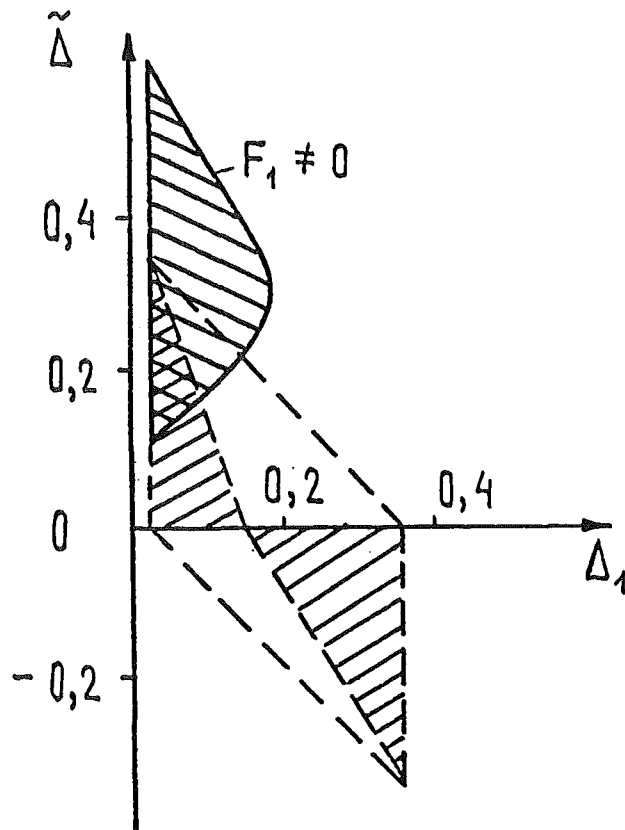


Fig. 14. Field of parasitic self excitation in the plane of mismatches Δ_1 , $\tilde{\Delta}$ in a nonexcited oscillator (dashed lines) and in a gyrotron with oscillation amplitude $F_1 \neq 0$ (shaded)

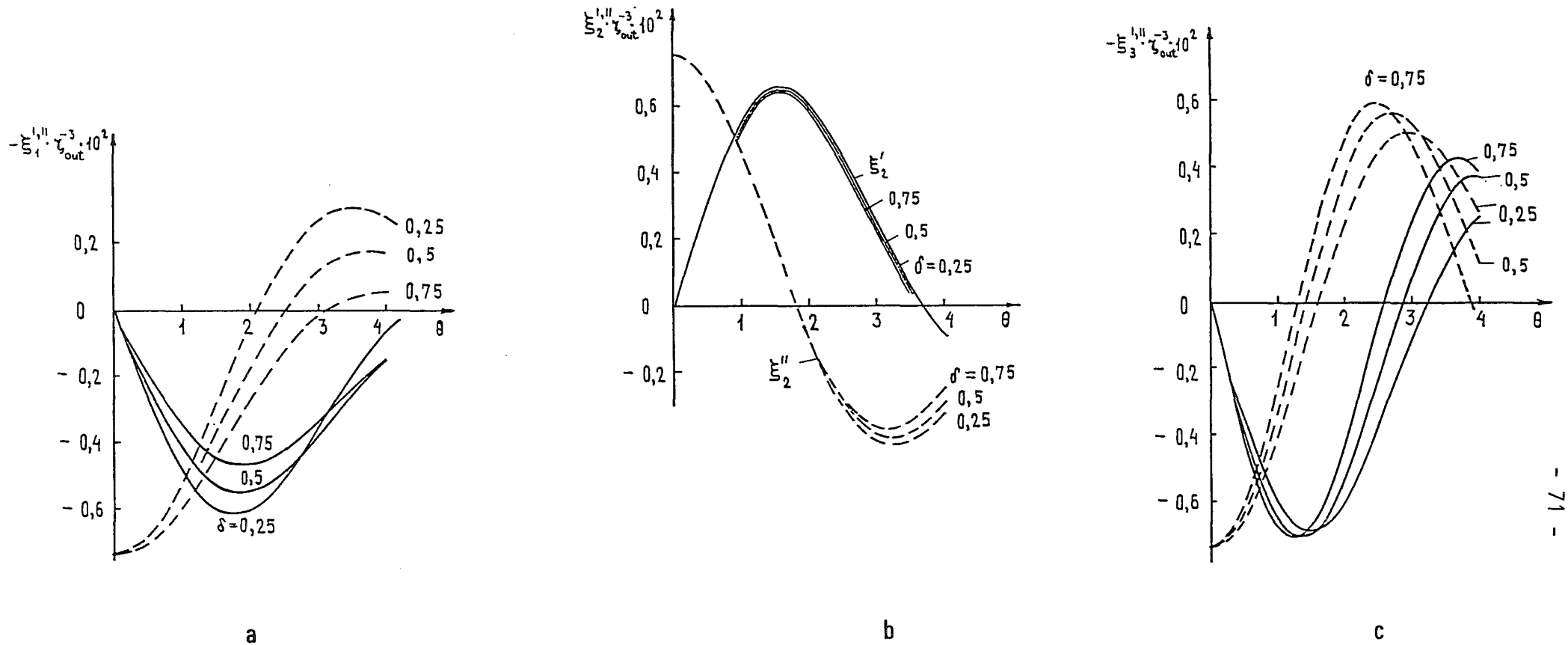


Fig. 15. Real (solid) and imaginary (dashed) parts of the coefficients ξ_s for a three mode gyrotron as a function of transit angle θ_2 for three values of $\delta = (\omega_2 - \omega_1) / (\omega_2 - \omega_{H_0})$ (mode 2 is the central mode) and constant field profile. (a) $s=1$; (b) $s=2$; (c) $s=3$

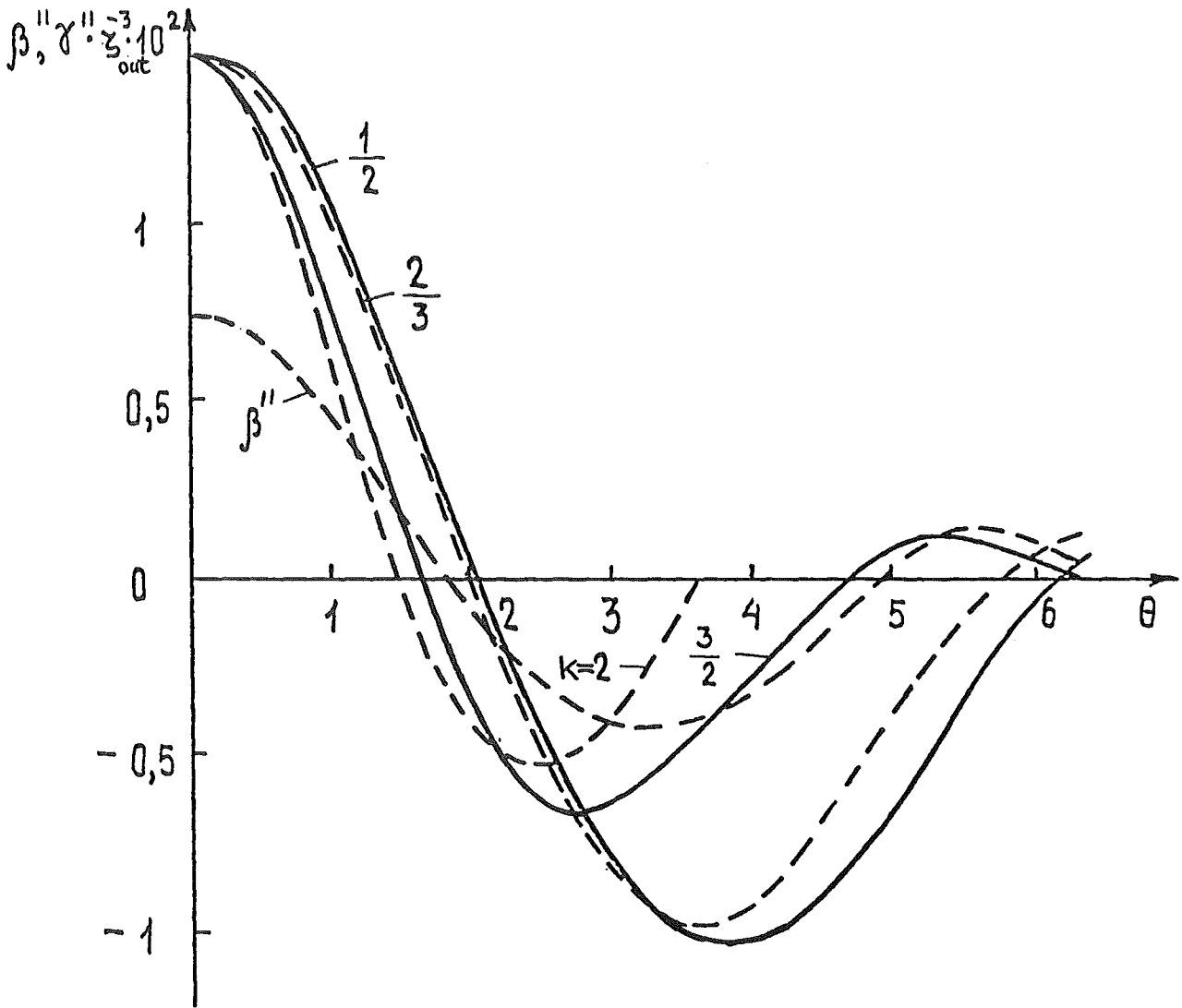


Fig. 16. Dependence of the coefficients γ_{ss} , and β_s on transit angle θ_2 for different values of the ratio $K = \theta_{s1} / \theta_s$.

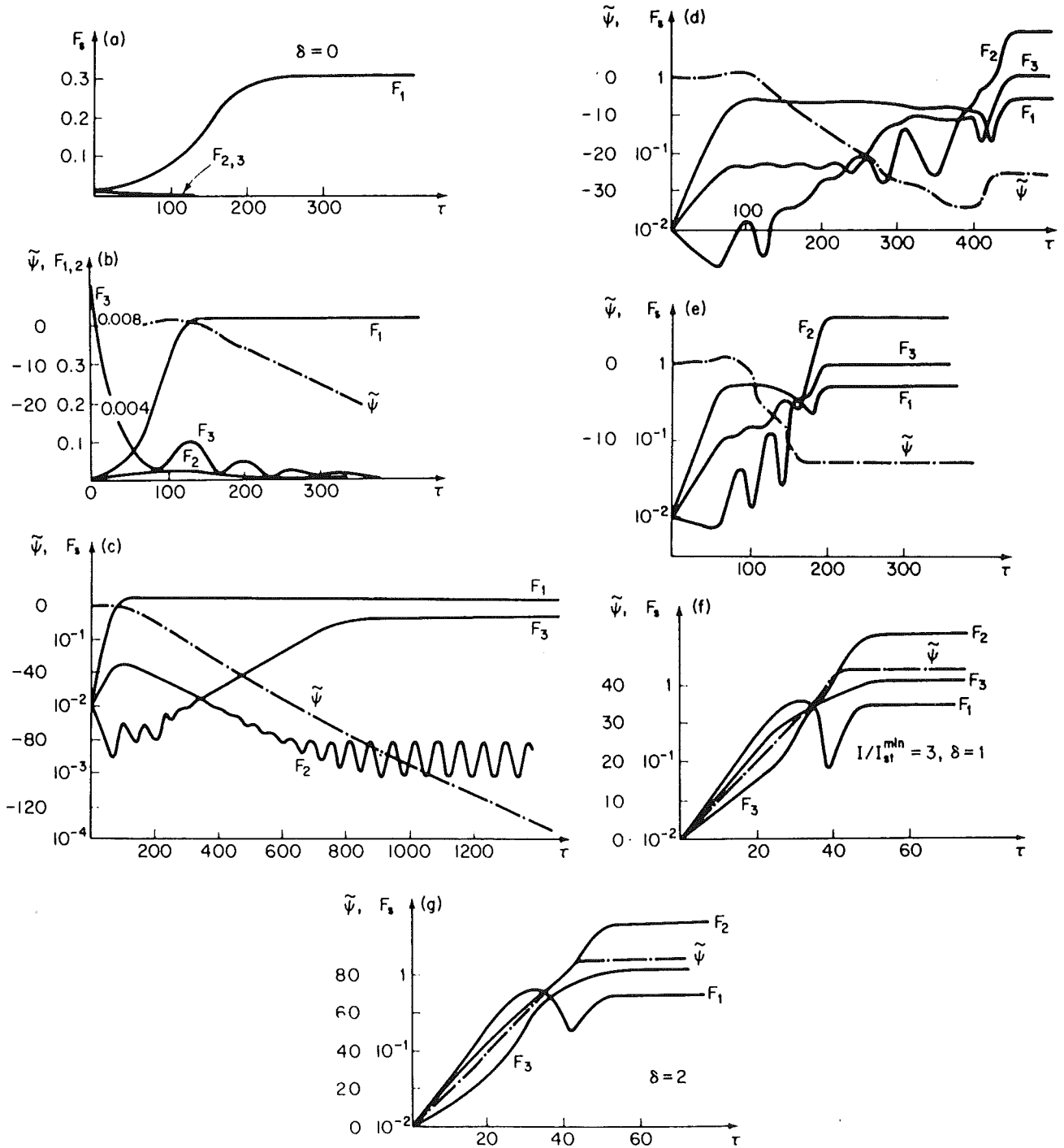


Fig. 17. Amplitude and phase time evolution in a three mode gyrotron with relation between modes. a) $I/I_{st}^{min} = 1.1, \delta = 0$; b) $I/I_{st}^{min} = 1.2, \delta = 0$; c) $I/I_{st}^{min} = 1.25, \delta = 0$; d) $I/I_{st}^{min} = 1.3, \delta = 0$; e) $I/I_{st}^{min} = 3.0, \delta = 0$; f) $I/I_{st}^{min} = 3.0, \delta = 1$; g) $I/I_{st}^{min} = 3.0, \delta = 2$.

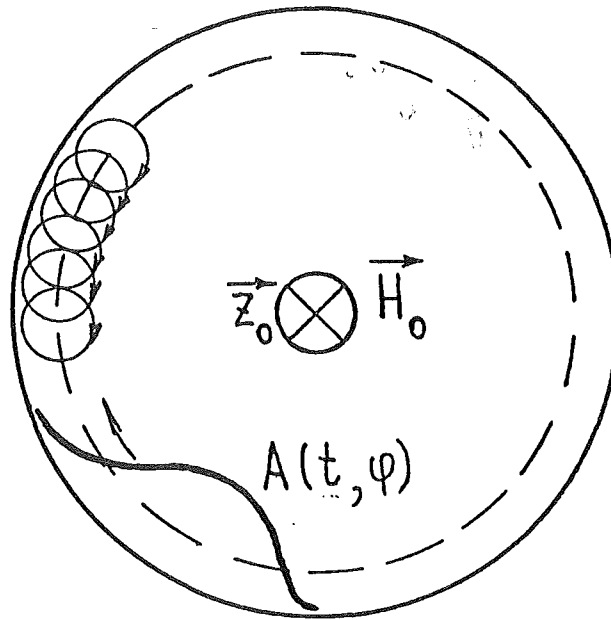


Fig. 18. Cross section of a CRM showing rotating wave envelope A defined in lecture 4.

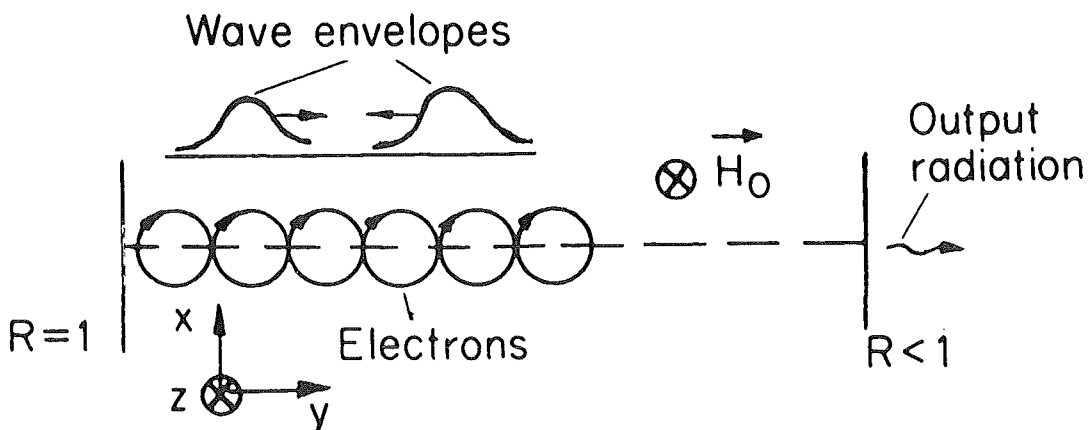


Fig. 19. Cross section of a CRM with counter-rotating waves in plane geometry.

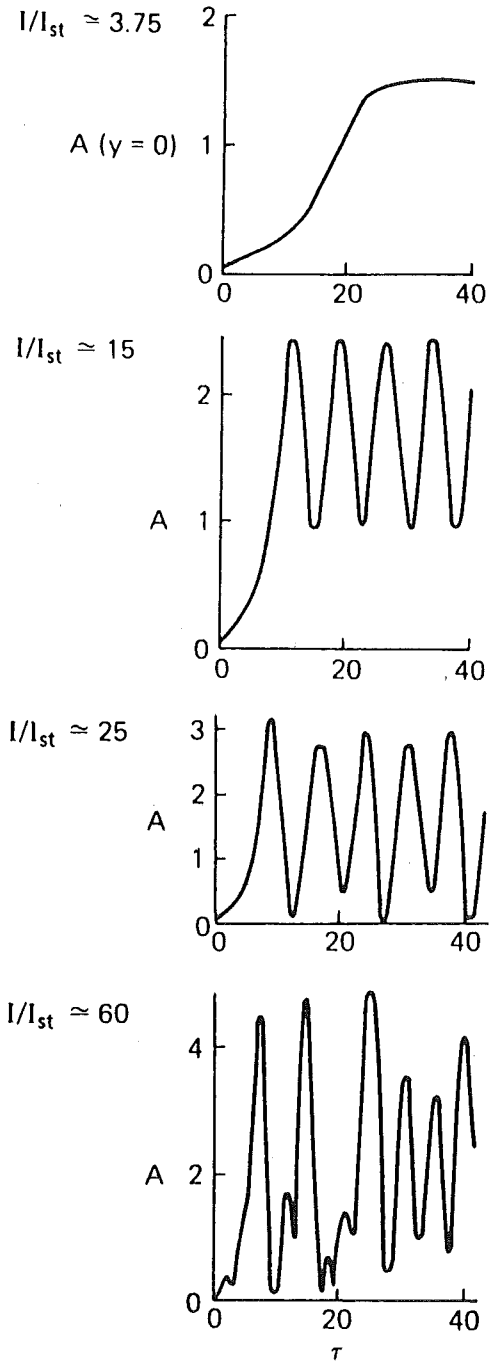


Fig. 20. Time dependence of the wave amplitude at the left mirror for various values of the beam current variable.

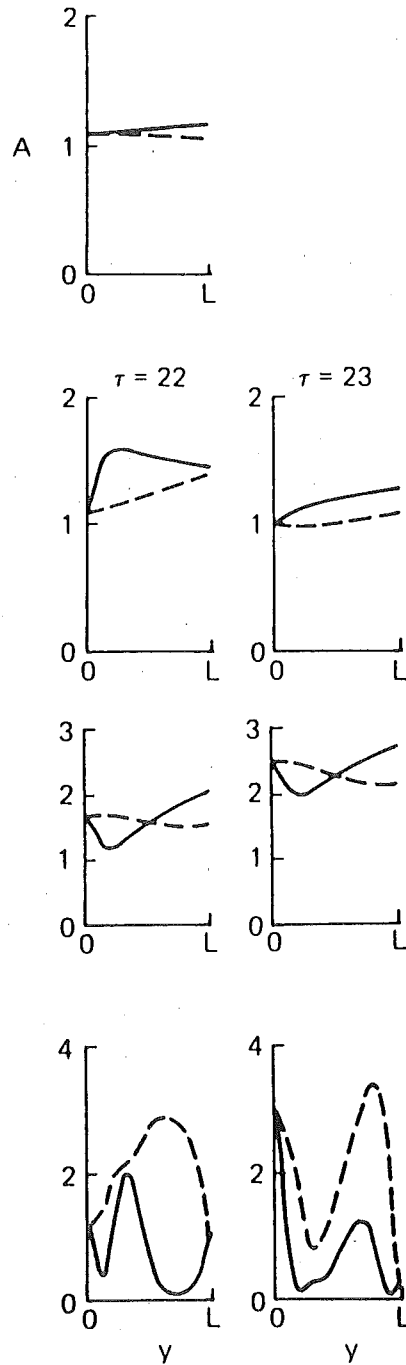


Fig. 21. Spatial structure of both opposite waves at fixed moments in time $\tau = I\omega t$ for various values of the beam current variable.

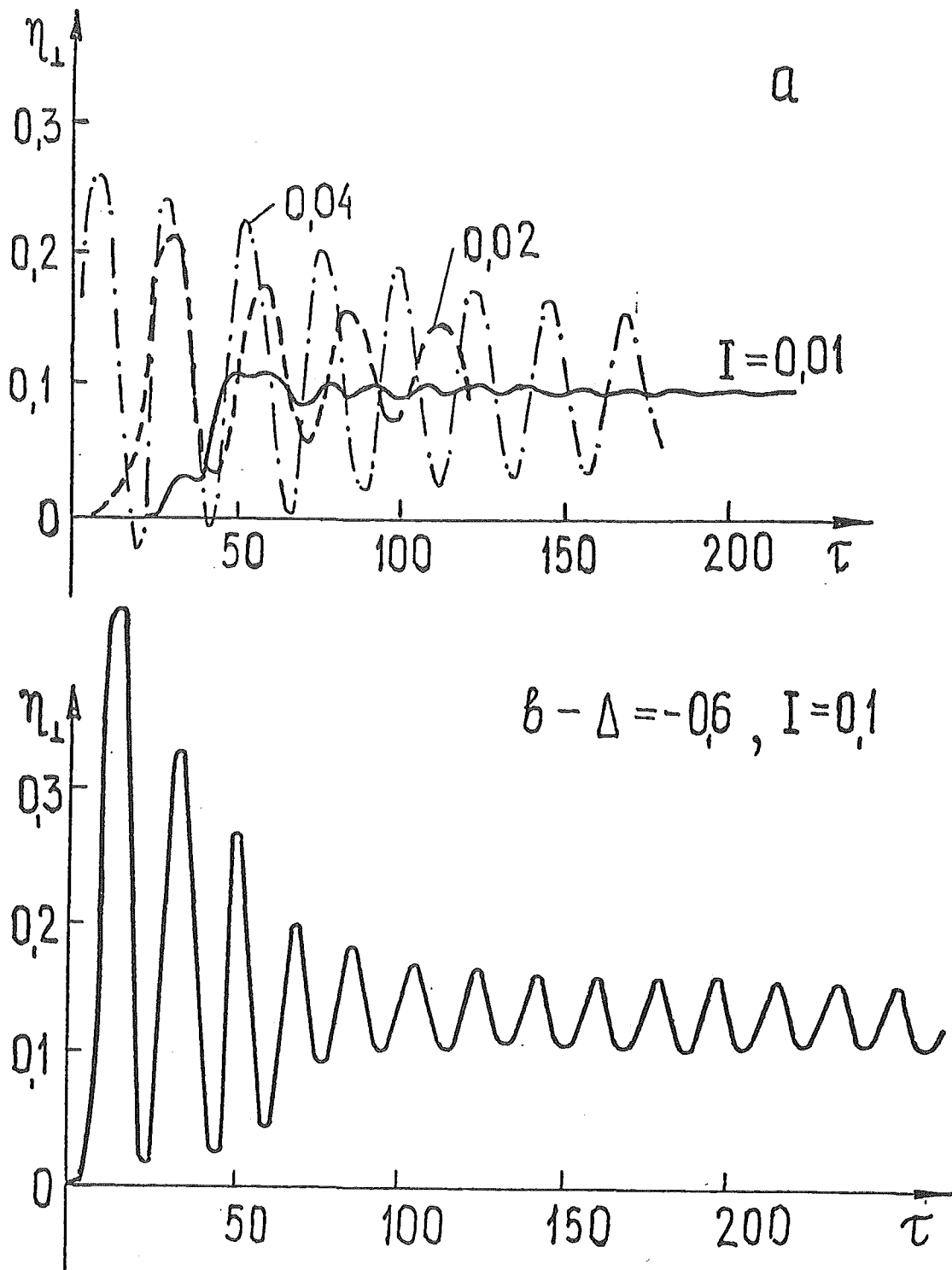


Fig. 22. Time dependence of efficiency for various values of beam current parameter with $\beta - \Delta = -0.6$ and $\zeta_{out} = 10$.

(a) $I=0.01, 0.02$ and 0.04 , showing the increase in duration of the nonstationary phase with increasing beam current.

(b) $I=0.1$, showing the onset of automodulation oscillations.

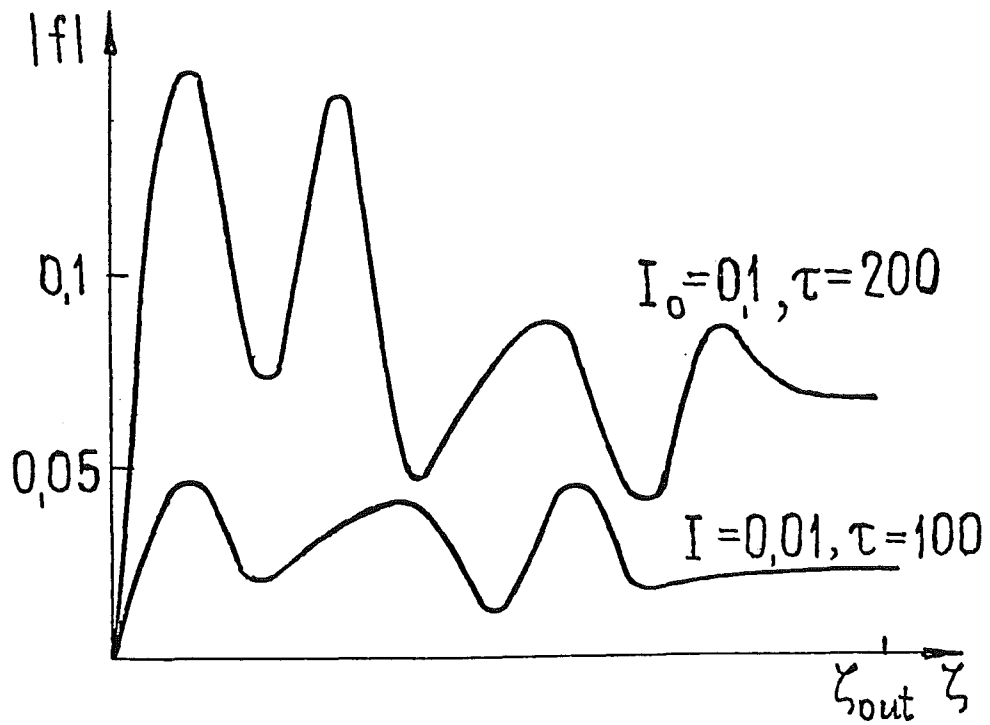


Fig. 23. Axial structure of resonator field at large values of the beam current parameter.